Measurements of Vibrational Power Transmission from Ship Main Engine

VÄRE Technology Programme, Tekes

VTT TECHNICAL RESEARCH CENTRE OF FINLAND

VTT INDUSTRIAL SYSTEMS

A	Work report	
B	Public research report	X
	Research report, confidential to	

Title

Measurements of Vibrational power transmission from Ship Main Engine

Customer or financing body and order date/No.	Research report No.
Väre Technology Programme, Tekes	BVAL35-021224
Project	**Project No.**
Liikkuteho	V9SU00184
Author	**No. of pages/appendices**
Seppo Aatola	38 / -

Keywords

Vibrational power transmission, Vibration measurements, Structure-borne sound, Source characterisation

Summary

This experimental study belongs to the VÄRE subproject Vibration and noise control of transport equipment and mobile work machines. Literature review, which preceded this experimental study, was aimed to find methods for the characterisation of diesel engine of a ship as structure-borne sound source and to find design methods to minimise the sound transmission from machine via foundation to the ship structure. The aim of this experimental study was to apply and take into use the characterisation methods found in literature. Method was selected after literature survey without any experimental pre-tests. With this method it is possible to determine vibrational power transmission from vibrating source to the surrounding structure using measured vibration data. Method is based on measured mechanical driving-point mobility, transfer mobility and vibration velocities of the surrounding structure in the "far-field". Vibrational power transmission was successfully calculated from measured signals. However, quite large discrepancy existed between powers calculated with two different ways. According to the literature review this method has been applied to rather small structures. Large discrepancy mentioned above might be due to large and complicated real-life structure. However, the method seems to be promising and probably results could be improved by optimising excitation equipment for large and heavy structures.

Date Espoo 4 November 2002

Pekka Koskinen	Seppo Aatola	
Deputy Research Manager	Senior Research Scientist	Checked

Distribution (customers and VTT):

VTT TECHNICAL RESEARCH CENTRE OF FINLAND
VTT INDUSTRIAL SYSTEMS
Tekniikantie 12, Espoo
P.O. Box 1705, FIN-02044 VTT
FINLAND
Tel. +358 9 4561
Fax +358 9 455 0619
name.surname@vtt.fi
www.vtt.fi/tuo
Business ID 0244679-4

Foreword

VÄRE - Control of Vibration and Sound - Technology Programme 1999-2002 is a national technology programme launched by the National Technology Agency (Tekes). It raises the readiness of companies to meet the stricter demands set by market for the vibration and sound properties of products.

As to structure-borne sound power and the characterisation of machines as a source of structure-borne sound there are not yet generally accepted international standards or methods. The research work on these topics is going on both in theoretical and practical aspects. Instead the properties of machines as a source of air borne sound are well established and standardised internationally.

This project is subproject of Vibration and noise control of transport equipment and mobile work machines, which belongs in VÄRE Technology Programme mentioned above. This project is financed by Tekes, VTT Manufacturing Technology (nowadays VTT Industrial Systems) and Finnish companies: diesel engine manufacturer Wärtsilä NSD Finland Oy (nowadays Wärtsilä Finland Oy), ship yards Kvaerner Masa-Yards Inc. and Aker Finnyards Ltd.

Tapio Hulkkonen from Kvaerner Helsinki yard leaded the supervising group from the beginning to 10th of November 2000. Thereafter Peter Sundström from Wärtsilä Finland Oy took the leadership. The other members of the supervising group were: Jouko Virtanen, Berndt Lönnberg and Juhani Siren from Kvaerner; Jukka Vasama, Kari Kyyrö and Jari Lausmaa from Aker Finnyards; Petri Aaltonen from Wärtsilä; Teijo Salmi, project manager of subproject "Vibration and noise control of transport equipment and mobile work machines", from VTT Industrial Systems and Matti K. Hakala, project director of the VÄRE Technology Programme, from VTT Industrial Systems.

The author wants to express his warm thanks to the supervising group for the support and encouragement during the work, and to all who helped with measurements both in Rauma and in Turku and also during sea voyage.

Espoo 24.5.2002

Seppo Aatola

Table of contents

1 Introduction

Literature survey of estimation methods of vibrational power flow preceded this experimental study [1]. Estimation method presented by Ohlrich [2] was selected to be used in this study. This method has been successfully used for example with receiver in the form of a ship model engine foundation [2] and with 3/4-scale helicopter fuselage [2].

It was decided to apply the method, "Ohlrich-method", to ship hull and main propulsion engine in full-scale.

11000 DWT Ro-Ro carrier build by Aker Finnyards Oy Finland (see cover picture) which has two main propulsion engines type W9L46C build by Wärtsilä NSD Finland, was selected as research object.

2 Goals

Goal of these vibration measurements was to find out the applicability of the estimation method of vibrational power transmission presented in [2]. Applicability was aimed to find out in the ship context in full-scale.

3 Theory

Ohlrich [2] has presented methodology how to determine vibrational power transmission from vibrating source to the surrounding structure using measured vibration data. This method is based on measured mechanical driving-point mobility, transfer mobility and vibration velocities of the surrounding structure in the "far-field". This method is reviewed in more detail in [1].

Properties of the vibration transfer path as a black box should be known prior to the determination of vibrational power transmission. Properties of transfer path can be examined by calibrating the receiver before installation of the source. Calibration will be done by giving broad-band force excitation into the representative mounting points of the source and following should be measured: driving-point mobility, transfer mobility between the representative receiver points and driving points, and vibration velocities of the receiver points during broad-band force excitation. This is expressed in equation (1) [2]:

$$P = \left\langle v_q^{\,2} \right\rangle \left\langle \frac{\mathrm{Re}\left(Y_{R,ii}\right)}{\left\langle \left| Y_{R,qi} \right|^2 \right\rangle} \right\rangle_i \qquad (1)$$

where P is power, v is velocity, Re is real part of ( ), Y is mobility, subindex R represent receiver, subindex q represent receiver point, subindex i represent excitation point.

Brackets in equation (1) mean spatial average. The latter term in brackets can be considered as calibration term, which is frequency dependent. This term is said to be robust and insensitive to variations in driving point properties and forcing directions [2].

However, often the source is already installed at the time of vibration measurements and therefore equation (1) cannot be applied. Therefore approximate expressions of a form similar to equation (1) are derived [2]. Determination of power flow with source installed need, adding to the functions mentioned above, that also either source mobility or receiver mobility is known at the selected representative mounting points. Expression of vibrational power transmission when source mobility is known is as follow [2]:

$$P \approx \left\langle v_q^{\,2} \right\rangle \left\langle \frac{|Y_{ii}|^2 \,\mathrm{Re}\left(1/Y_{ii} - 1/Y_{S,ii} \right)}{\left\langle |Y_{qi}|^2 \right\rangle} \right\rangle_i \qquad (2)$$

where P is power, v is velocity, Re is real part of ( ), Y is mobility, subindex S represent source, subindex q represent receiver point, subindex i represent excitation point.

3.1 Method used in this study

The method presented in [2] was used. This method was applied to real ship, i.e. all measurements were done in full-scale. Main engine of the ship was regarded as vibration source and ship hull was regarded as receiver of vibration. The ship was brand new and ready to sail. Main engines were already installed and therefore equation (2) was applied. Four excitation points and eight receiver points in "far-field" were used for estimation of vibrational power transmission.

4 Description of the ship

M/S Norstream is an 11000 DWT Ro-Ro carrier built by Aker Finnyards Oy. Length of the vessel is approximately 168 m and breadth approximately 25 m. Bridge and cabins are situated in forepart of the ship (see cover picture). This vessel has two four-blade propellers, which can be powered independently. These main propulsion engines are type W9L46C (nr.91084 and 91085, main engines nr.1 and 2, respectively) built by Wärtsilä Finland Oy. Running speed of these engines is 500 rpm and rated power at this speed is 9450 kW; thereby total power is 18.9 MW. Gearboxes (nr.43426 and 43427) are type M1BHC-1100+S650 built by Valmet company in Finland. Transmission ratio of these gearboxes is 3. Engines are mounted rigidly to the rigid engine foundation of the ship (see figure 4).

Measurements with resiliently mounted engine: Engine type W9L46D (nr.91386) with running speed of 514 rpm and rated power 10395 kW.

5 Measurements

5.1 Measurements in the ship

Measurements were carried out on board M/S Norstream, ship of Bore shipowners, at the harbour of Aker Finnyards in Rauma and during her sea voyage from city of Rauma in Finland to city of Teesport in UK.

In the ship all vibration measurements were carried out around main engine nr.2 which is situated on right-hand side of the ship (starboard, SB). Two types of measurements were carried out. First shaker excitation was given into four excitation points (EP, see table 1), one at a time. Driving-point mobility and transfer mobility were measured as well as vibration responses simultaneously from eight measuring points (MP, see table 2) around the main engine nr.2. Secondly vibration responses from the same eight measuring points were measured both during idling of main engine nr.2 and during sea voyage when both main engines were running synchronously at same load (50%, 85% and 95%). Layout of after-body of the ship is seen in figure 1.

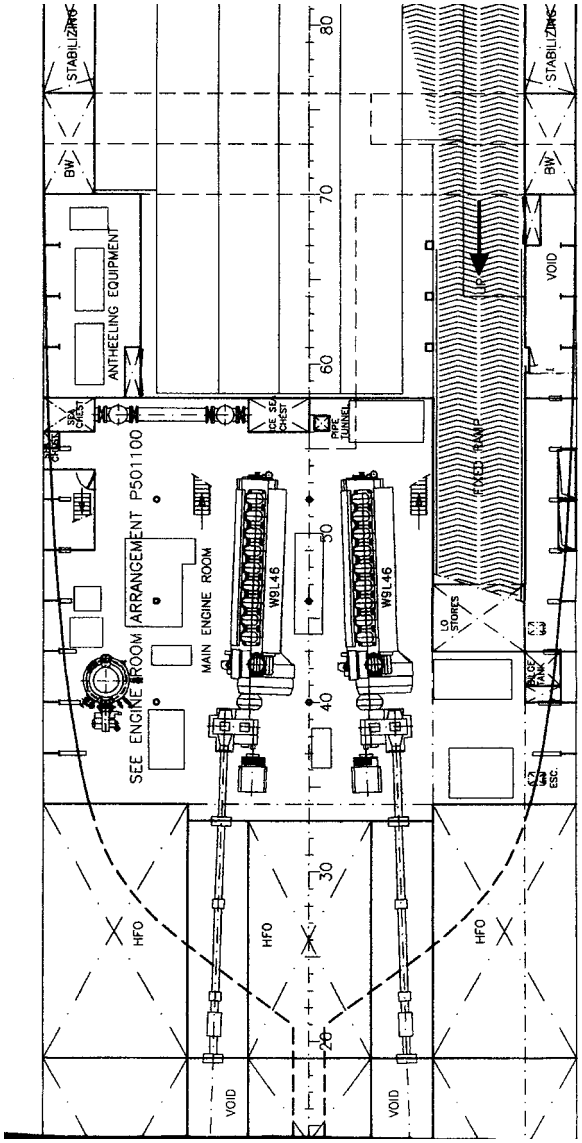

Figure 1. Layout of after-body of the ship.

5.1.1 Measuring points

Locations of the four excitation points are described in table 1. Excitation points SB11 and SB13 are seen in figures 2 and 5, respectively.

Locations of the eight measuring points are described in table 2. Measuring point SB1 is seen in figure 3.

Table 1. Locations of excitation points (EP) on the mounting base of the main engine (see also figure 2).

	distance from the side of the engine		between transversal bays**	distance from front-end of the engine *
EP	from sb-side (mm)	from bb-side (mm)	(nr/nr)	(mm)
SB11	270	-	#44/#45	-6550
SB12	320	-	#51/#52	-1015
BB13	-	200	#51/#52	-1000
BB14	-	175	#45/#46	-6000

* negative: to aft-direction of the ship
sb, starboard, right-hand side of the engine
bb, portside, left-hand side of the engine
** distance between transversal bays is 800 mm

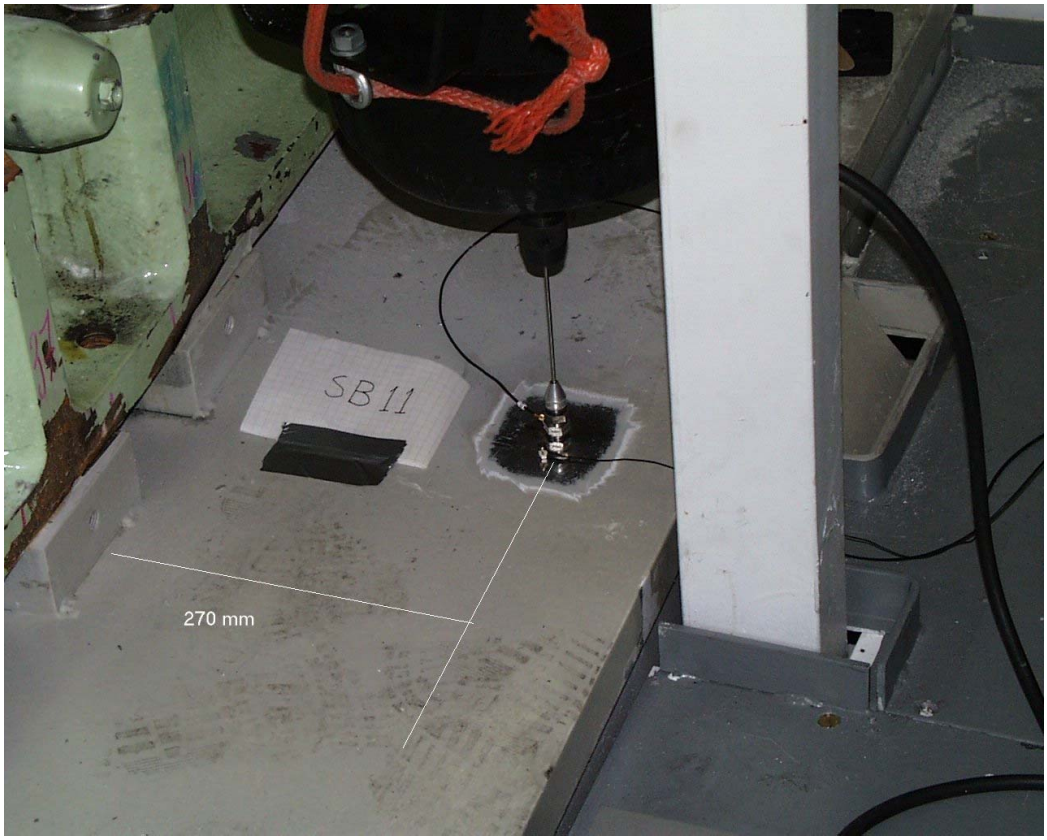

Figure 2. Vertical excitation with electrodynamic shaker (excitation point SB11).

Table 2. Locations of measuring points (MP) on the cover plate below mounting base level of the main engine (see also figure 3).

	distance from longitudinal bay alongside the engine		between	distance from transversal bay	
MP	SB (mm)	BB (mm)	transversal bays** (nr/nr)	bay (nr)	distance* (mm)
SB1	215	-	#40/#41	#40	210
SB2	200	-	#43/#44	#43	205
SB3	265	-	#48/#49	#49	-195
SB4	250	-	#51/#52	#52	-235
BB5	-	670	#51/#52	#51	240
BB6	-	515	#48/#49	#49	-315
BB7	-	255	#43/#44	#43	270
BB8	-	235	#41/#42	#41	280

* positive: to bow-direction of the ship

* negative: to aft-direction of the ship

SB, starboard, right-hand side of the engine

BB, portside, left-hand side of the engine

** space between transversal bays is 800 mm

Figure 3. Measuring point SB1; accelerometer glued to the target (mounting base level of the main engine nr.2 is seen at the upper left corner of the photograph).

Longitudinal section of the main engine mounting bed (foundation) is seen in figure 4.

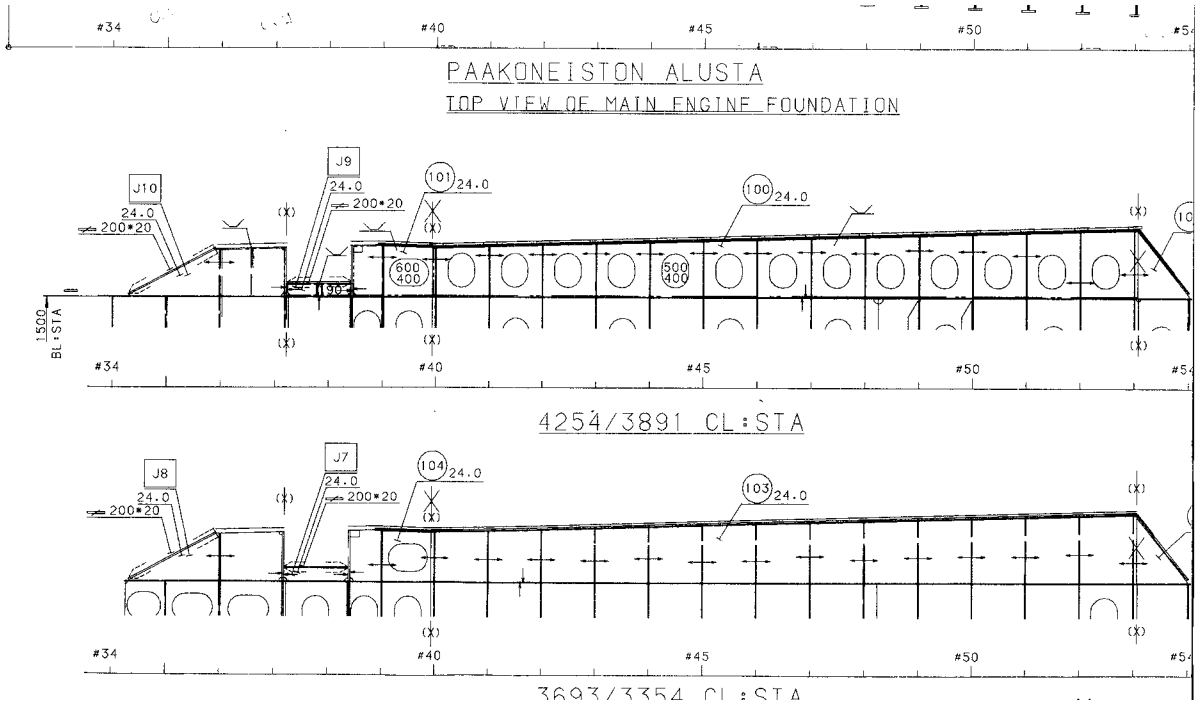

Figure 4. Mounting bed of main engine, longitudinal section.

5.1.2 Measuring equipment

Vibration was measured with piezoelectric accelerometers and excitation force with piezoelectric force transducer. Signals were captured and analysed with multi-channel signal analyser. Measuring equipment is listed in table 3. In addition, some set-up parameters are listed in table 3.

TABLE 3. Measuring equipment in the ship.

Ch	Label	MP	Dir.	Sensor	EU	pC/EU	Amplifier	mV/EU
1	SB/1	1	+Z	BK4393/1	m/s2	0,317	BK2635/1	100
2	SB/2	2	+Z	BK4393/2	m/s2	0,315	BK2635/2	100
3	SB/3	3	+Z	BK4393/3	m/s2	0,318	BK2635/3	100
4	SB/4	4	+Z	BK4393/4	m/s2	0,315	BK2635/4	100
5	BB/5	5	+Z	BK4393/5	m/s2	0,316	BK2635/5	100
6	BB/6	6	+Z	BK4393/6	m/s2	0,315	BK2635/6	100
7	BB/7	7	+Z	BK4375/2	m/s2	0,317	BK2635/7	100
8	BB/8	8	+Z	BK4375/3	m/s2	0,317	BK2635/8	100
9	Excitation	*	+Z	BK4375/4	m/s2	0,316	BK2635/9	100
10	Excitation	*	+Z	BK8200/1	N	3,760	BK2635/10	10

* four driving-points, one at a time

Excitation: Shaker LING V455 with amplifier LING PA 1000

Signal Source: Source module of HP3566A/67A

Analyser: HP 3566A/67A
BK = Brüel & Kjær
HP = Hewlett-Packard

5.1.3 Shaker excitation

Mobility measurements, i.e. frequency response function (FRF) measurements using shaker excitation were carried out at the harbour of Aker Finnyards in Rauma during night 26.-27.11.1999. All engines of the ship were in stop-position and there was no other activity in the ship during these measurements. Excitation was given in vertical direction into four points on the mounting base of the main engine, into one point at a time (figure 5). Locations of these excitation points are given in table 1. Excitation was measured with force transducer, which was mounted to the structure by a screw (figure 5). Acceleration of the excitation point was measured with piezoelectric accelerometer (figure 5) which was mounted to the structure using beeswax. Response was measured with piezoelectric accelerometers simultaneously from 8 points around the main engine (four points on each side of the main engine nr.2); these accelerometers were glued to the structure. Locations of accelerometers are listed in table 2. All accelerometers and their amplifiers were same type of same manufacturer. Measuring equipment is listed in table 3.

Figure 5. Installation of shaker, engine bed with mounted engine in the ship (excitation point BB13).

Injected force during shaker excitation is seen in figure 6. According to the theory injected force should be broadband. Injected force was broadband only to some extent. Injected force was depending on frequency, it had two heavy peaks and it was above background level up to approximately 6500 Hz (see figure 6). Therefore estimation of power flow will be limited to the frequency of 6500 Hz.

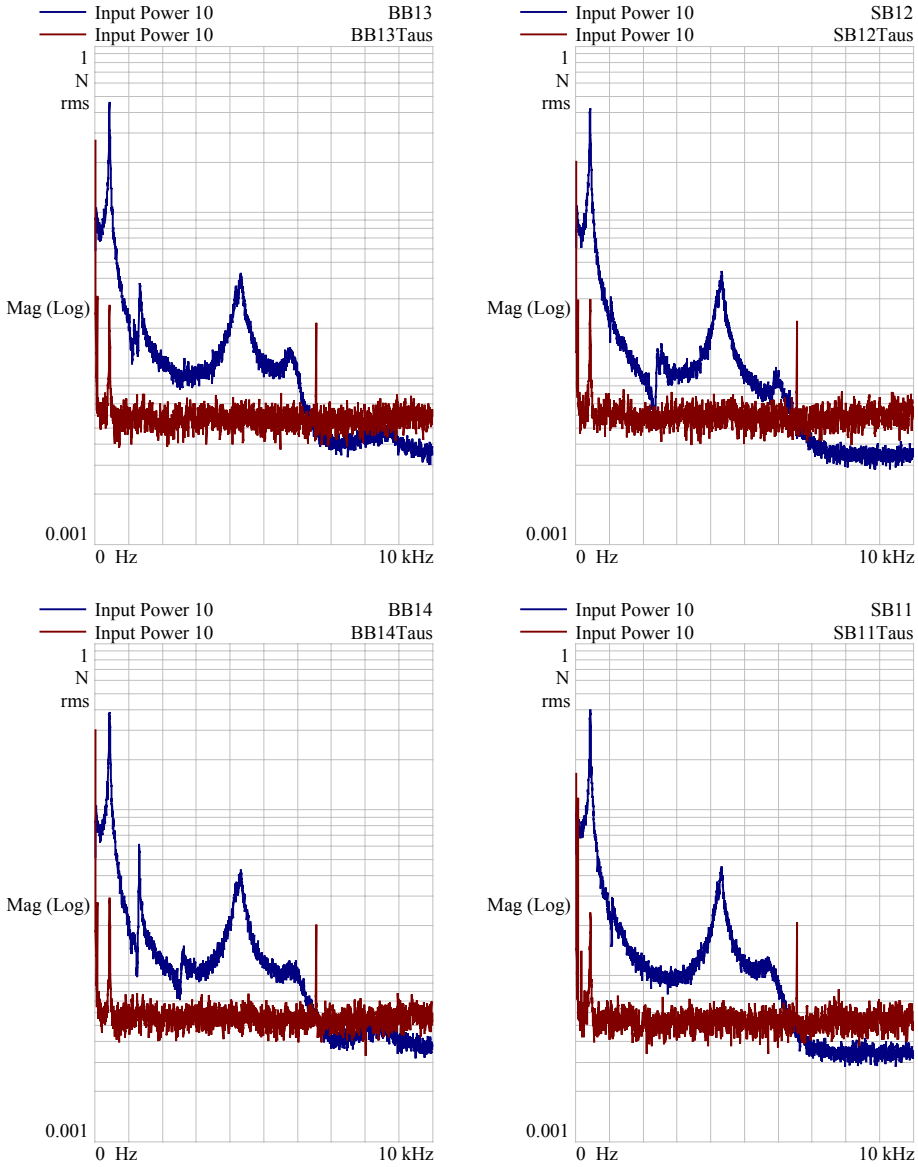

Figure 6. Spectra (linear frequency axis) of excitation force (N, rms, logarithmic axis) at excitation points SB11, SB12, BB13 and BB14 (blue curve); background noise (red curve).

Response in eight measuring points due to the shaker excitation is seen in figures 7-10 when excitation was given into point SB11, SB12, BB13 and BB14, respectively. Vibration response in these eight far-field points was quite small (figures 7-10). Vibration was highest around frequency of 400 Hz at level of approximately 0.01 m/s², rms. Vibration was above background level at most of the measuring points approximately up to 6500 Hz and therefore, as mentioned earlier, estimation of power flow will be limited to this frequency.

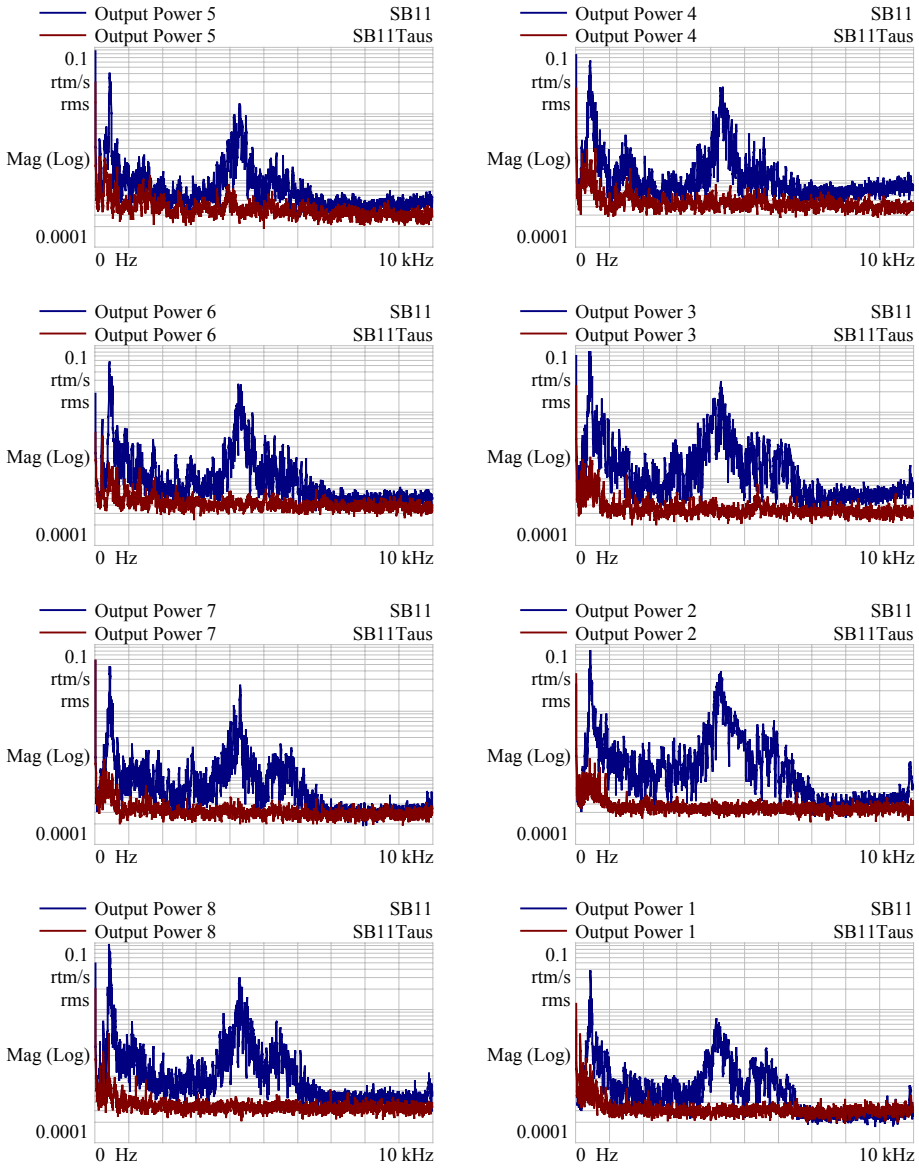

Figure 7. Vibration acceleration spectra (m/s², rms, logarithmic axis; linear frequency axis) at measuring points 1...8; shaker excitation in excitation point SB11 (blue curve); background noise (red curve).

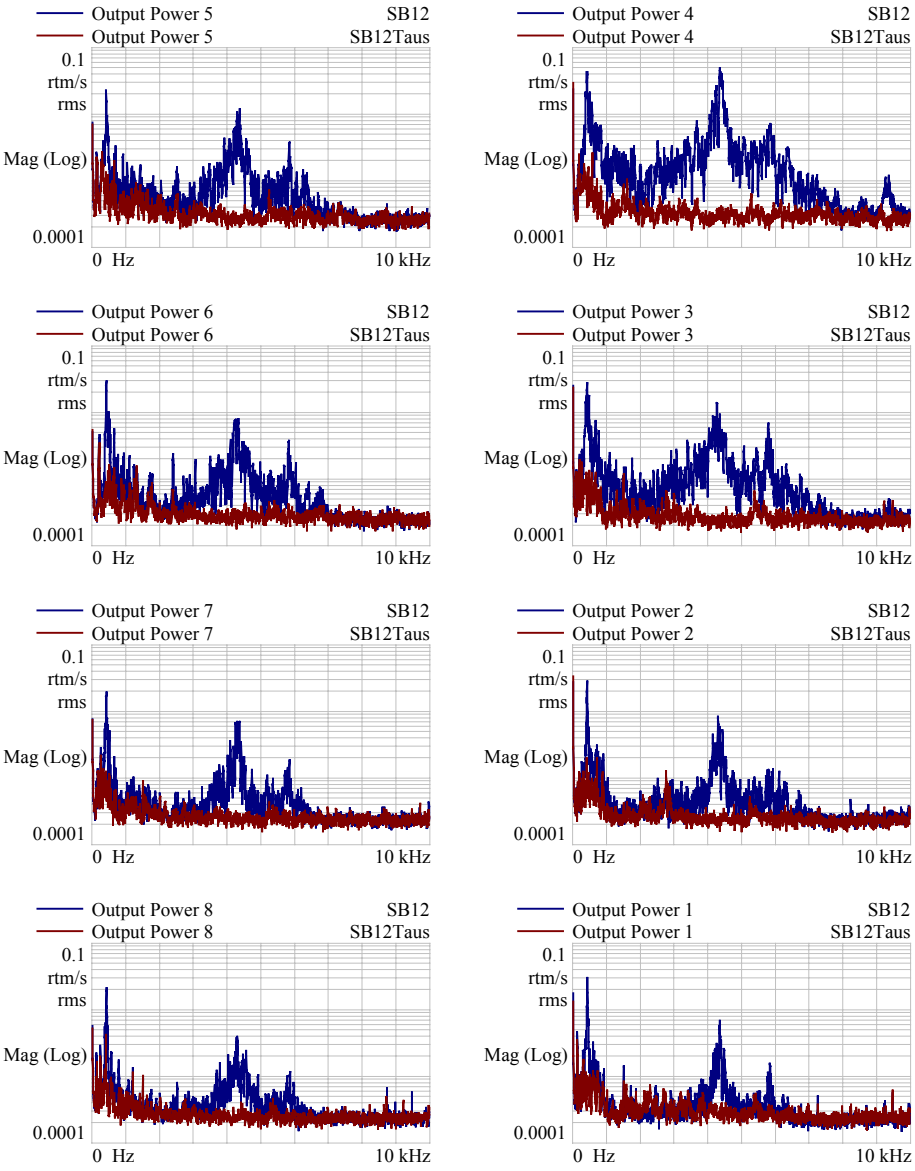

Figure 8. Vibration acceleration spectra (m/s², rms, logarithmic axis; linear frequency axis) at measuring points 1...8; shaker excitation in excitation point SB12 (blue curve); background noise (red curve).

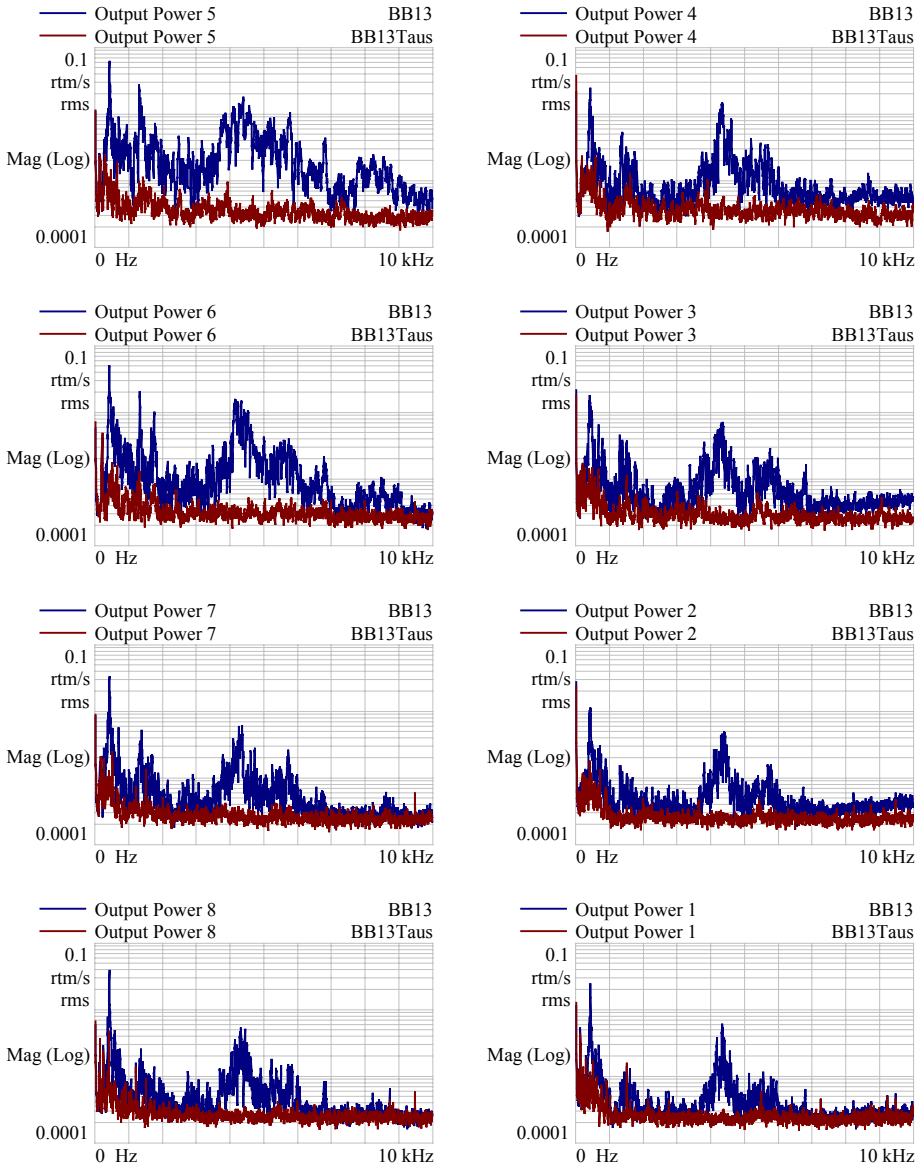

Figure 9. Vibration acceleration spectra (m/s², rms, logarithmic axis; linear frequency axis) at measuring points 1...8; shaker excitation in excitation point BB13 (blue curve); background noise (red curve).

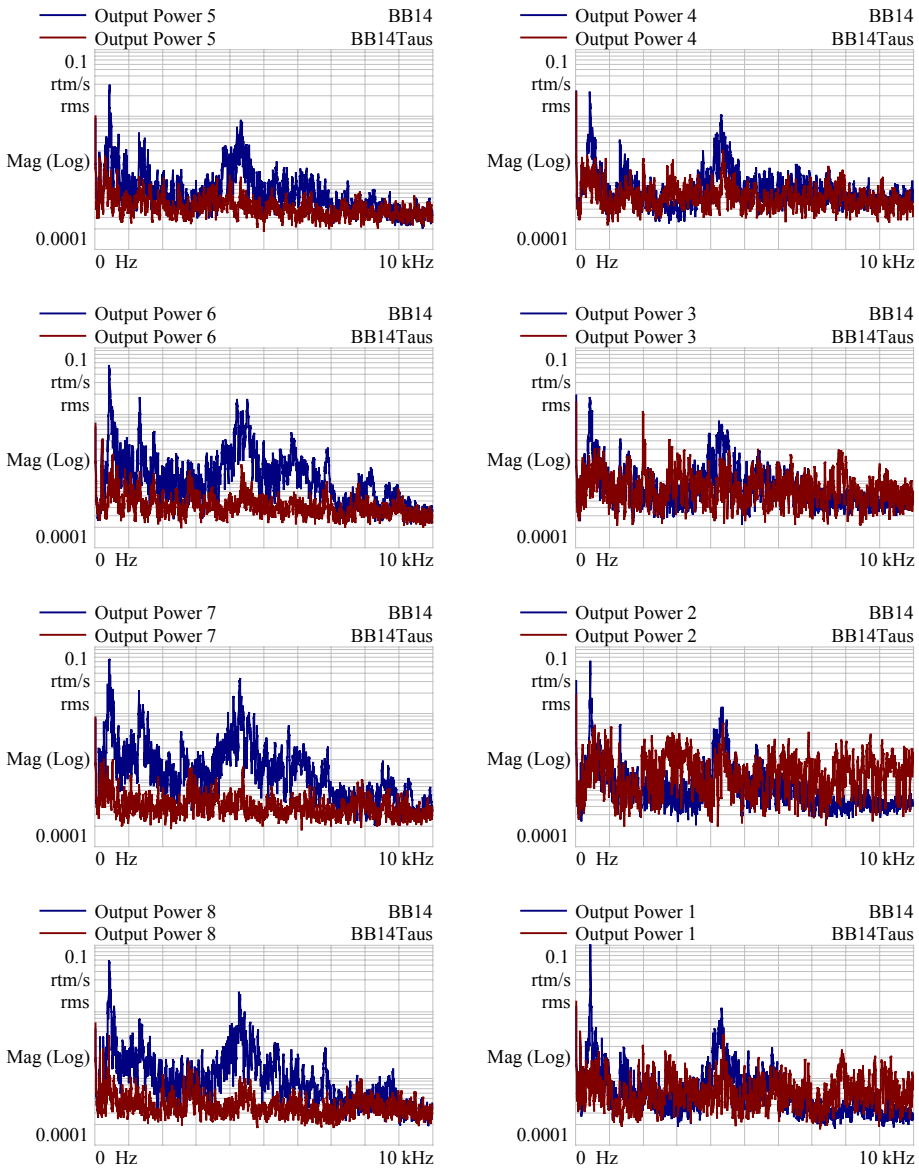

Figure 10. Vibration acceleration spectra (m/s², rms, logarithmic axis; linear frequency axis) at measuring points 1...8; shaker excitation in excitation point BB14 (blue curve); background noise (red curve).

Coherence between injected force and driving-point acceleration are seen are figure 11. Coherence during all four excitations is rather good between frequencies from 200 Hz and 6000 Hz.

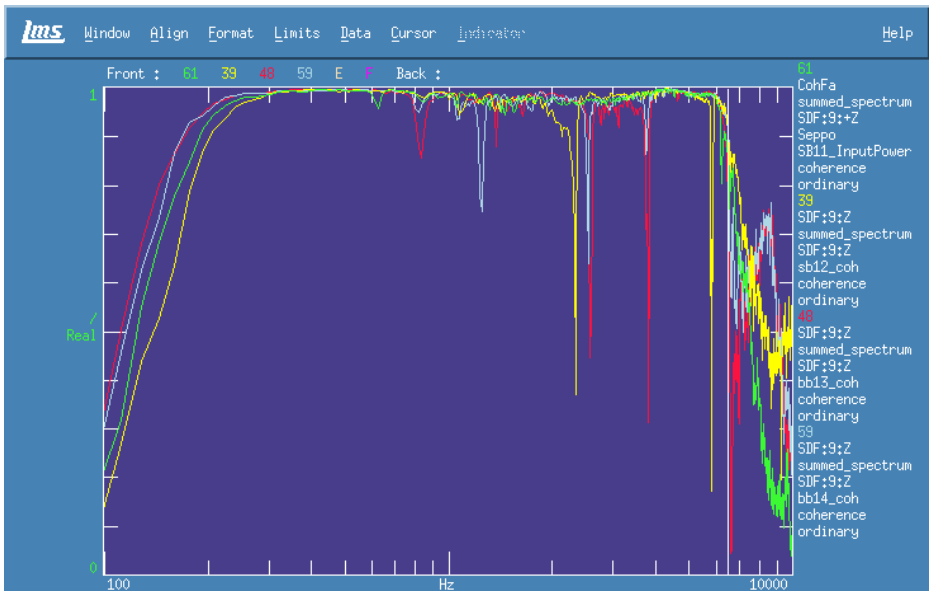

Figure 11. Coherence between injected force and driving-point acceleration of excitation point SB11 (green), SB12 (yellow), BB13 (red) and BB14 (blue) (logarithmic frequency axis).

Example of coherence between injected force and far-field accelerations are seen in figures 12 and 13 (excitation point SB12). Coherence is rather poor on the opposite side of the engine (figure 13) but rather poor also on the same side of the engine (figure 12). Presumably power calibration estimate will not be very accurate.

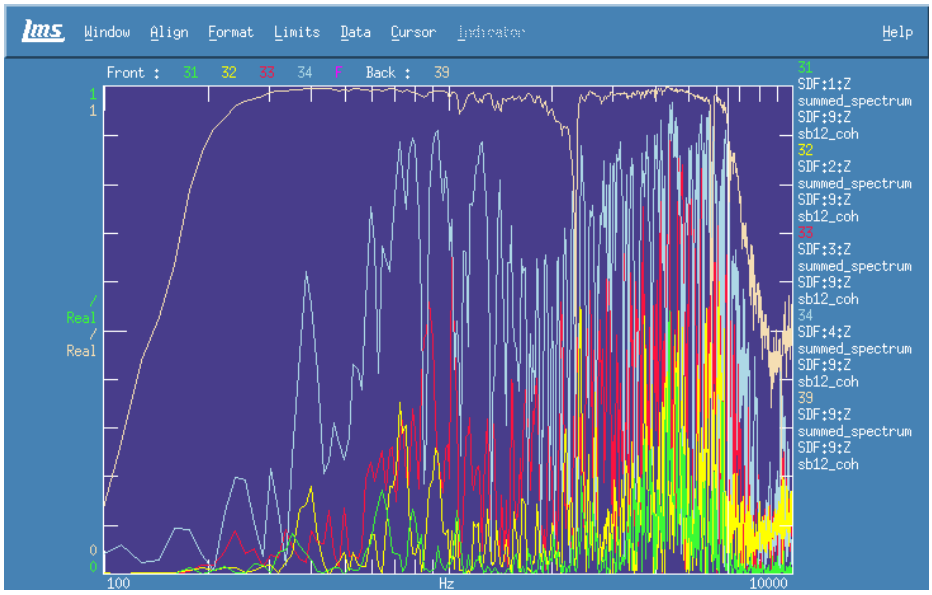

Figure 12. Coherence between injected force (SB12) and accelerations in far-field (MP 1-4); driving-point coherence also present (uppermost curve) (logarithmic frequency axis).

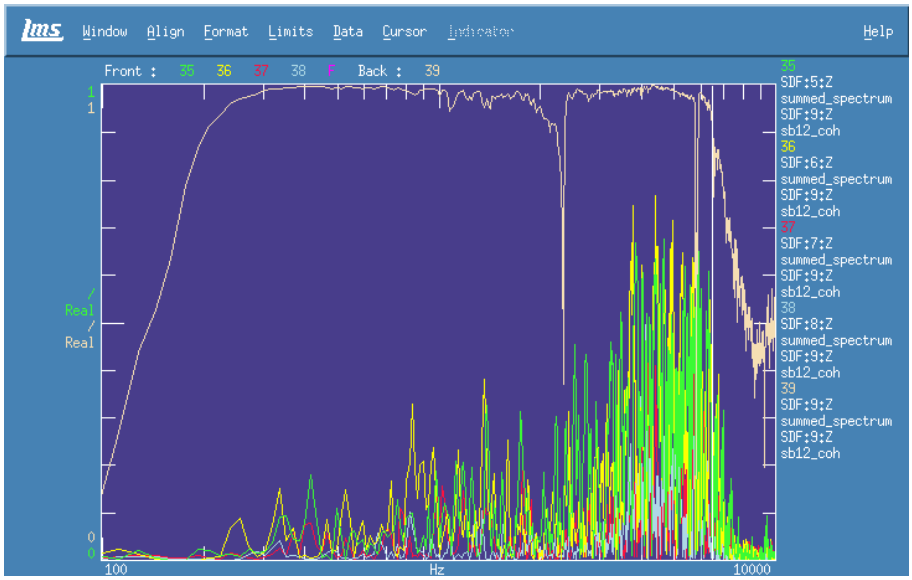

Figure 13. Coherence between injected force (SB12) and accelerations in far-field (MP 5-8); driving-point coherence also present (uppermost curve) (logarithmic frequency axis).

Average velocities of all eight far-field measuring points during excitations are seen in figure 14. Average velocity seems to be quite similar with all the excitations. However, small difference is seen between different sides of the engine approximately around frequency of 1400 Hz (figure 14). Therefore power calibration can be done using just data of two excitation points, one on each side of the engine. However, all excitation data was used in this study.

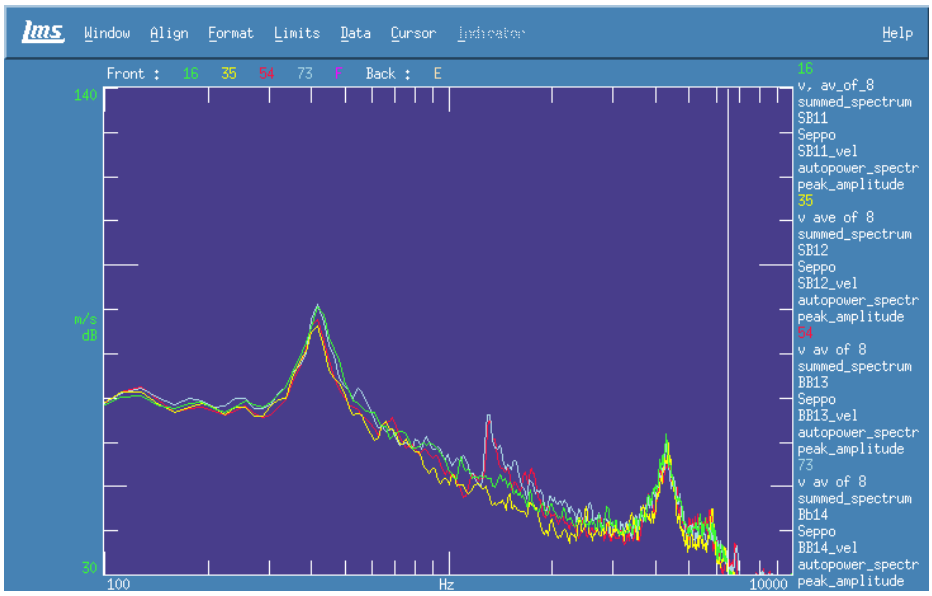

Figure 14. Average velocity spectra (dB, re 1e-9 m/s, logarithmic axes) of all eight measuring points in far-field during excitation of SB11 (green), SB12 (yellow), BB13 (red) and BB14 (blue).

5.1.4 Response during idling

Vibration measurements during idling of main engine nr.2 were carried out at the harbour of Aker Finnyards in Rauma 28.11.1999. Engine speed was 300 rpm and propeller has no pitch. All other engines of the ship were in stop-position during these idling measurements. Vibration at eight measuring points is seen in figure 15. Vibration was highest between frequencies from 0 Hz to 100 Hz and was approximately at level of 1 m/s², rms.

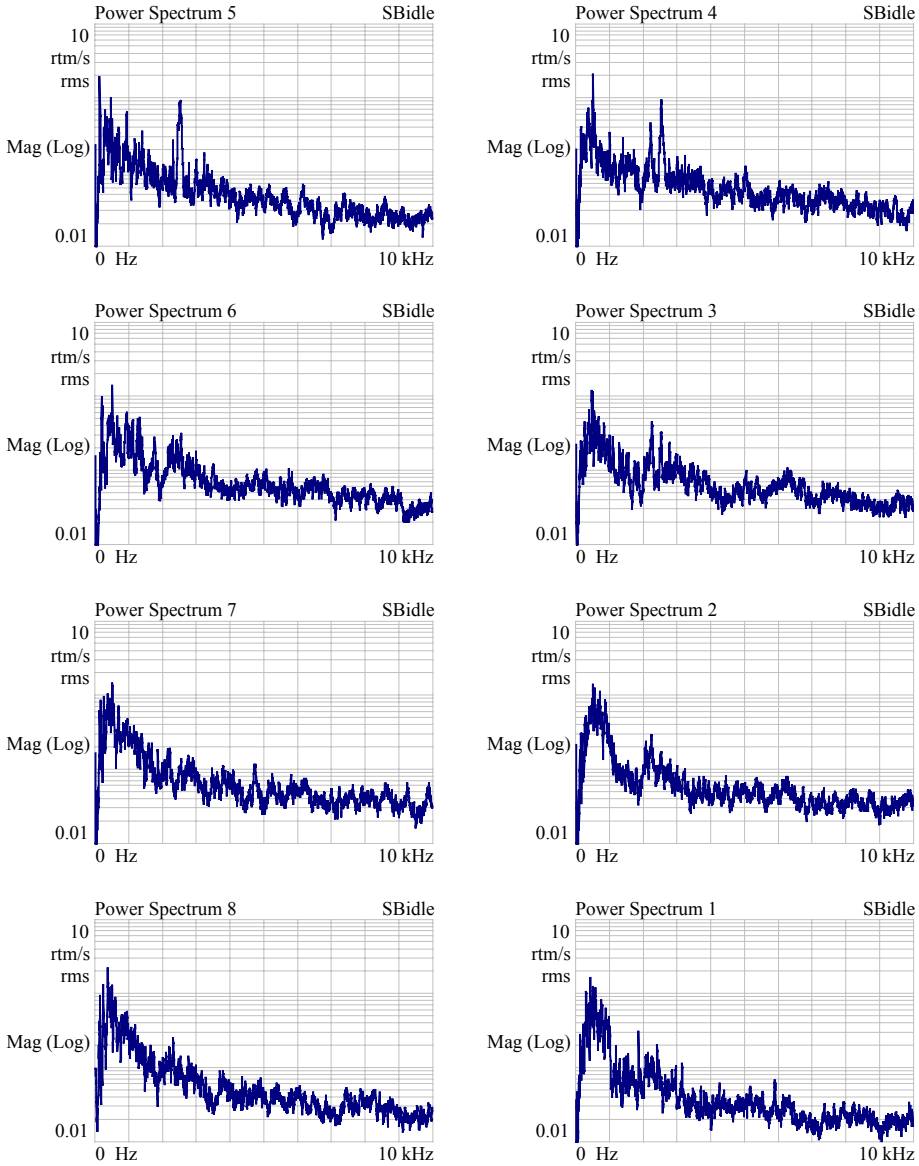

Figure 15. Vibration acceleration spectra (m/s², rms, logarithmic axis; linear frequency axis) at measuring points 1...8 during idling.

5.1.5 Response during sea voyage

Measurements under three operational loads were carried out on Baltic Sea during sea voyage from city of Rauma in Finland to city of Teesport in UK 29.11.1999. Operational loads of both main engines were 50%, 85% and 95% and running speed of the engines was 490 rpm. Baltic Sea was quite calm during measurements. Ship had no cargo during this voyage. Response in eight measuring points is seen in figures 16-18 when engine load was 50%, 85% and 95%, respectively. Vibration was highest between frequencies from 0 Hz to 100 Hz and was approximately at level from 2 m/s² to 5 m/s², rms.

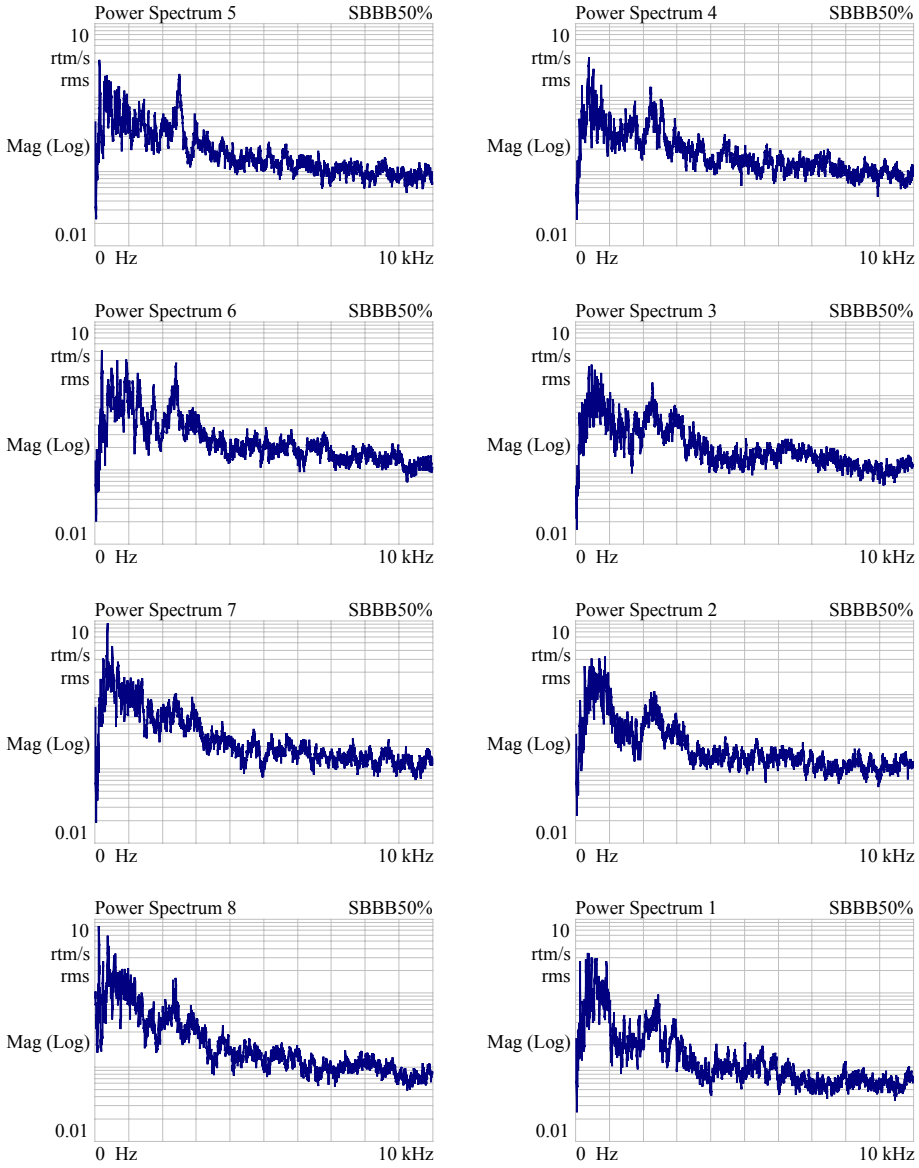

Figure 16. Vibration acceleration spectra (m/s², rms, logarithmic axis; linear frequency axis) at measuring points 1...8 with operational load of 50% during sea voyage.

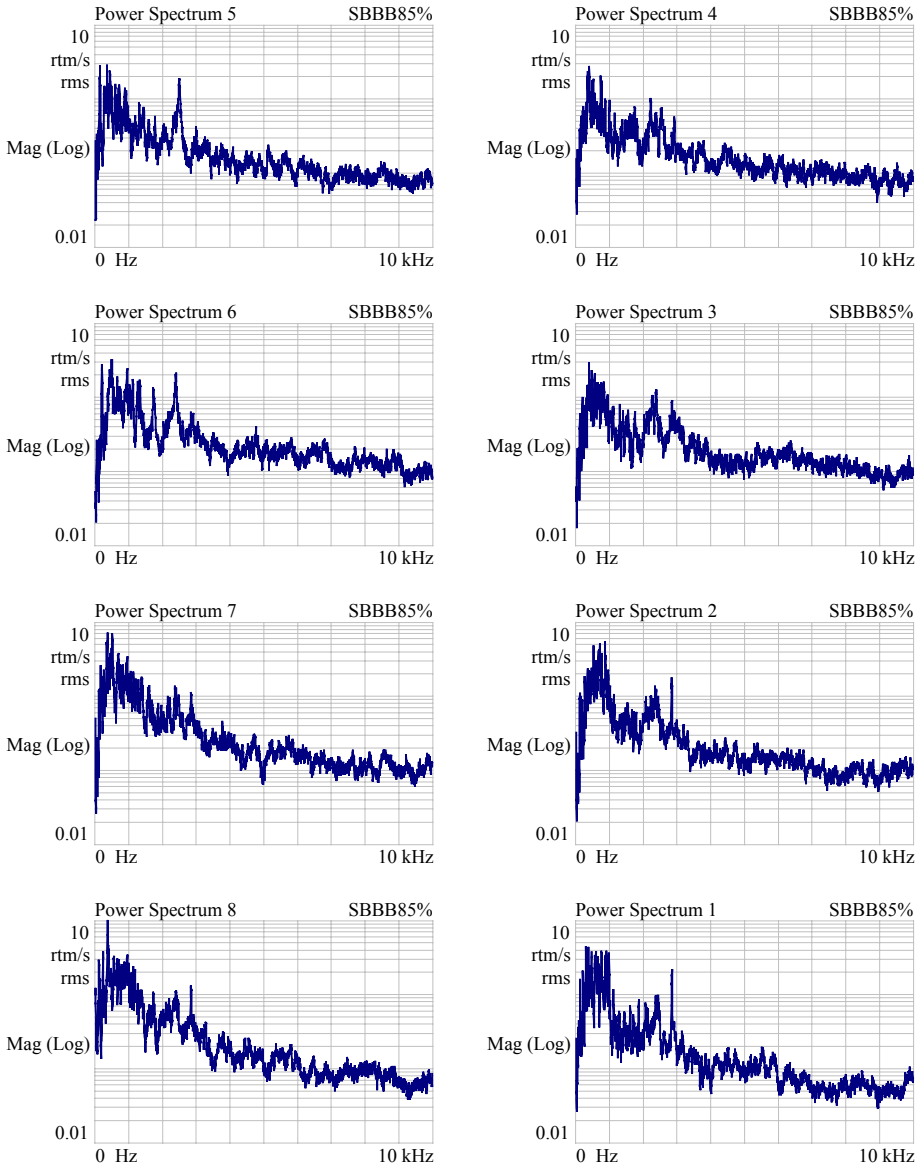

Figure 17. Vibration acceleration spectra (m/s², rms, logarithmic axis; linear frequency axis) at measuring points 1...8 with operational load of 85% during sea voyage.

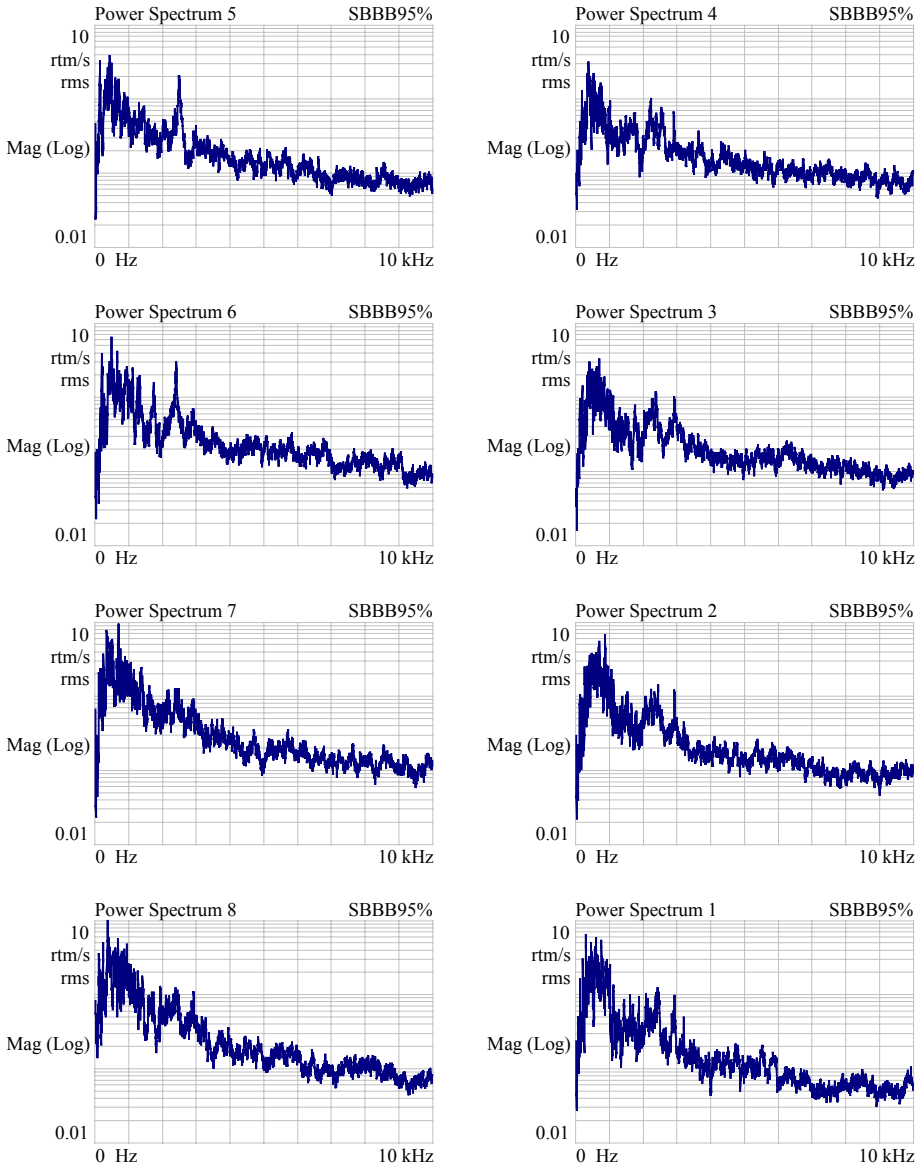

Figure 18. Vibration acceleration spectra (m/s², rms, logarithmic axis; linear frequency axis) at measuring points 1...8 with operational load of 95% during sea voyage.

Average response of eight measuring points are seen in figure 19 when engine load was zero (idling), 50%, 85% and 95%. Average response increased with the load. However, difference between loads was rather small and nearly zero at frequencies above 1000 Hz. Average response of idling was approximately 10 dB below the other responses almost at all frequencies.

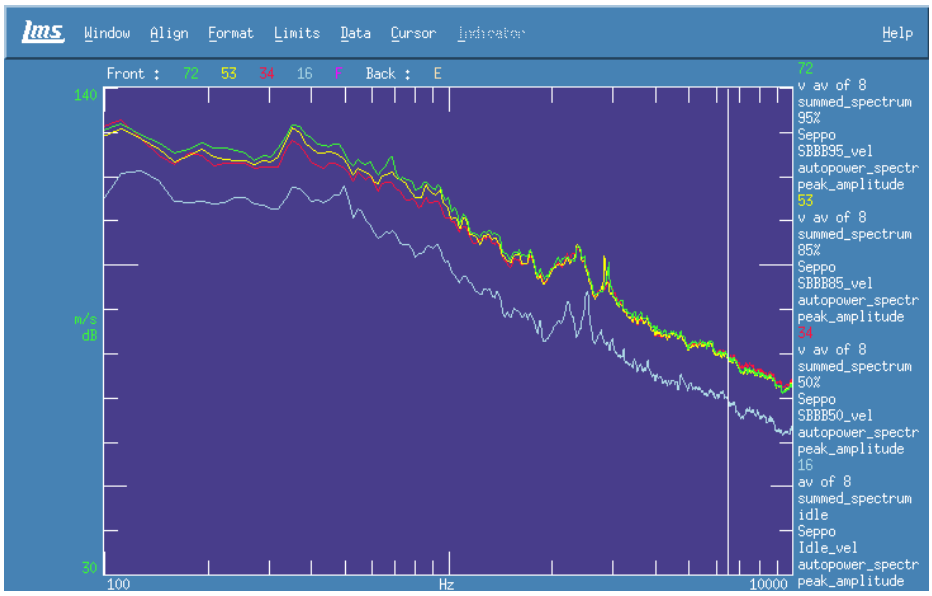

Figure 19. Average velocity spectra (dB, re 1e-9 m/s, logarithmic axes) of all eight measuring points in the far field during load of 95% (green), 85% (yellow), 50% (red) and idling (blue).

5.2 Measurements of resiliently mounted engine

Diesel engine W9L46C (nr.91386), similar to the engine in the ship, was measured later at test site of Wärtsilä in Turku. Mobility of resiliently mounted engine was measured near the points where shaker excitation was given in earlier mobility measurements in the ship. Engine was disconnected from outside world during these measurements; i.e. fuel hoses, exhaust pipes, cooling water pipes and gearbox were not connected to the engine.

Two types of measurements were carried out. Firstly vibration excitation was given into four excitation points in the engine, one at a time (shaker-points in figure 20). Two types of impact hammer were used as well as electrodynamic shaker (table 5) to determine driving-point mobility of the engine. Secondly vibration responses from ten measuring points were measured when the engine was running with steady loads of 85%, 90%, 100% and 110%. Responses were also measured from the engine foundation (bed) underneath the measuring point of engine. However, vibrations in all three directions (X, Y and Z) were only measured with load of 85%; with other loads vibration was measured only in vertical direction (Z).

5.2.1 Measuring points

Locations of the four excitation points and ten measuring points are seen in figure 20.

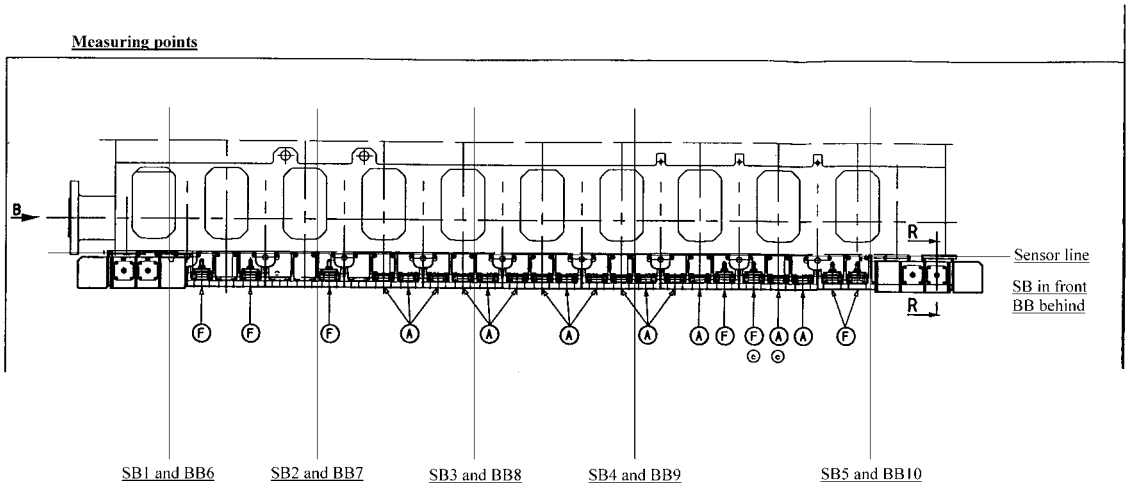

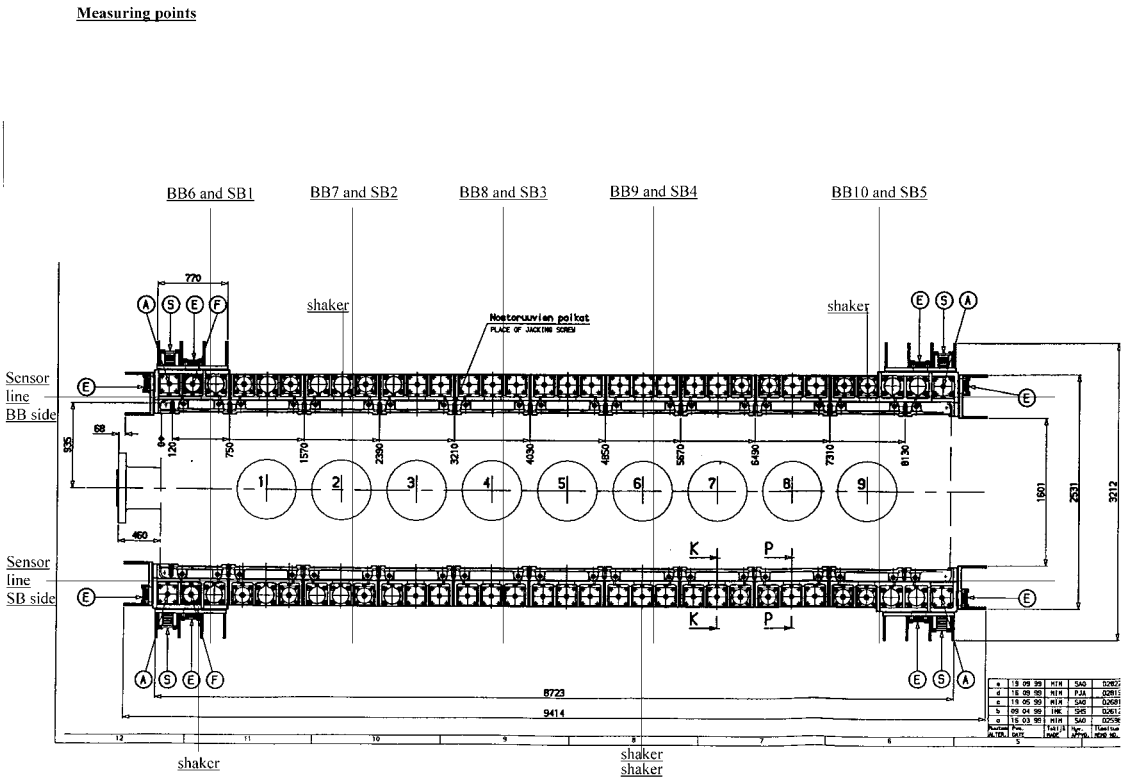

Figure 20. Measuring points 1-10 (BB and SB) and four excitation points (shaker); side view (upper picture) and top view (lower picture).

5.2.2 Measuring equipment

Vibration and excitation forces were measured with similar equipment than in the ship (see paragraph 5.1.2). However, some other type of accelerometers was used. Measuring equipment is listed in table 4 and 5. In addition, some set-up parameters are listed in these tables. All accelerometers and force sensor were mounted to the target using screw.

TABLE 4. Measuring equipment, resiliently mounted engine.

Ch	Label	MP	Dir.	Sensor	Output mV/ms-2
1	Engine/Bed *	1	X/Y/Z *	BK4395/1	0,986
2	Engine/Bed *	2	X/Y/Z *	BK4395/2	0,994
3	Engine/Bed *	3	X/Y/Z *	BK4395/3	0,993
4	Engine/Bed *	4	X/Y/Z *	BK4395/4	0,993
5	Engine/Bed *	5	X/Y/Z *	BK4395/5	0,997
6	Engine/Bed *	6	X/Y/Z *	E752-10/1	1,029
7	Engine/Bed *	7	X/Y/Z *	E752-10/2	1,015
8	Engine/Bed *	8	X/Y/Z *	E752-10/3	1,040
9	Engine/Bed *	9	X/Y/Z *	E752-10/4	1,035
10	Engine/Bed *	10	X/Y/Z *	E752-10/5	1,032

* one at a time

Analyser: HP 3566A/67A
BK = Brüel & Kjær
E = Endevco
HP = Hewlett-Packard

TABLE 5. Measuring equipment, mobility measurements of resiliently mounted engine.

Ch	Label	MP	Dir.	Sensor	Sensor	Amplifier	EU	Output mV/EU
low Freq								
1	hammer/ V8	drv-point	+Z	**K9361A**	4pC/EU	BK2635/5	N	1
2	engine	drv-point	+Z	BK4395/2	0,994mV/EU		m/s2	0,994
high Freq								
1	hammer/ V2	drv-point	+Z	**BK8200/1**	3,76pC/EU	BK2635/6	N	3,16
2	engine	drv-point	+Z	BK4395/2	0,994mV/EU		m/s2	0,994
1	shaker	drv-point	+Z	BK8200/3	3,88pC/EU	BK2635/6	N	10
2	engine	drv-point	+Z	BK4395/2	0,994mV/EU		m/s2	0,994

Excitation: Shaker LING V455 with amplifier LING PA 1000

Signal Source: Source module of HP3566A/67A

Analyser: HP 3566A/67A
BK = Brüel & Kjær
HP = Hewlett-Packard
K = Kistler

5.2.3 Shaker and impact hammer excitations

Mobility measurements of resiliently mounted engine using both shaker and impact hammer excitation were carried out at test site of Wärtsilä in Turku during night 12.-13.7.2001. There were no other activities in the factory during these measurements. Only air conditioning machine of the test site was operating during measurements. Excitation was given in vertical direction into four points on the mounting base of the main engine, into one point at a time (figure 21). Excitation was given and measured with responses similarly than in the ship (see paragraph 5.1.3). However, also impact hammers were used to see if FRF at high frequencies could be improved. Locations of these excitation points are given in figure 20 and measuring equipment is listed in table 5.

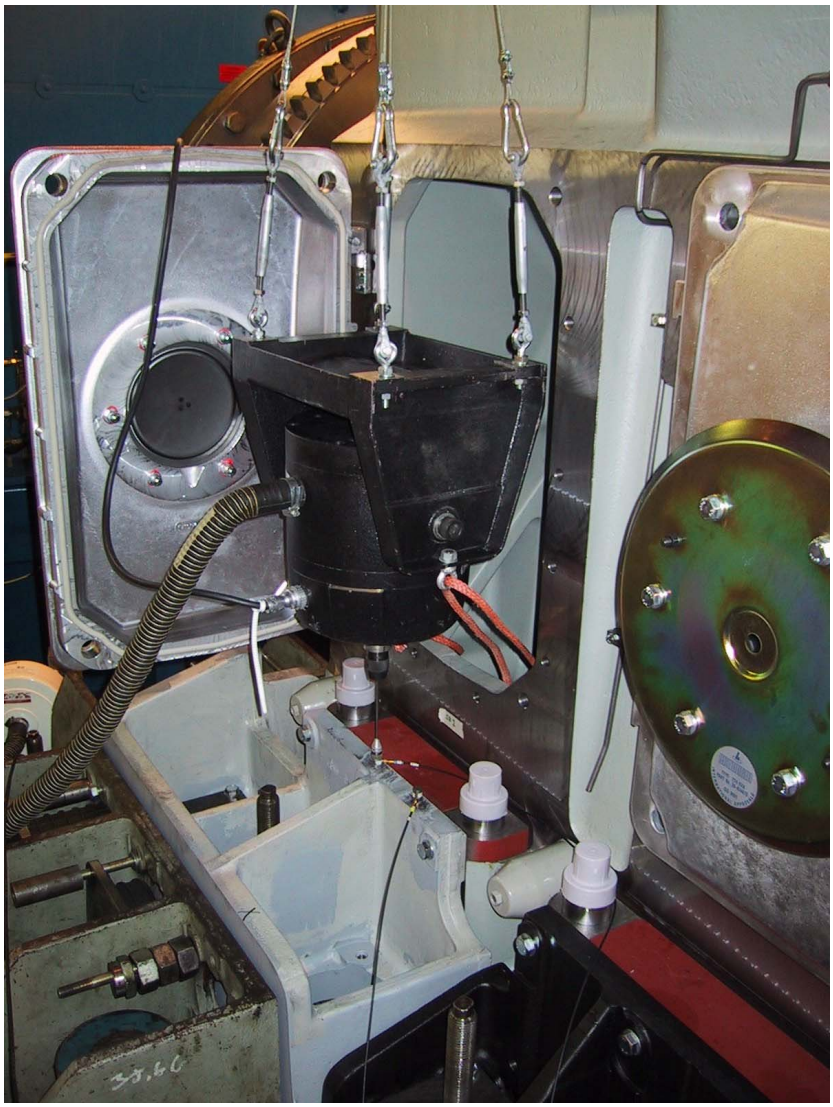

Figure 21. Installation of shaker, resiliently mounted engine (excitation point SB1).

Driving-point mobility achieved with three different excitation devices is seen in figure 22. Excitation devices were shaker and two type of custom made impact hammers (see table 5). Light hammer and shaker gave similar estimate approximately between frequencies from 250 Hz and 5500 Hz but large differences were seen at some frequencies (figure 22). Heavy impact hammer and shaker gave similar estimate approximately between frequencies from 100 Hz and 4100 Hz but large differences were found at some frequencies (figure 22). As a conclusion FRFs achieved with shaker excitation were selected to be used in further computations. Consistency with further computations in all was other reason for this selection.

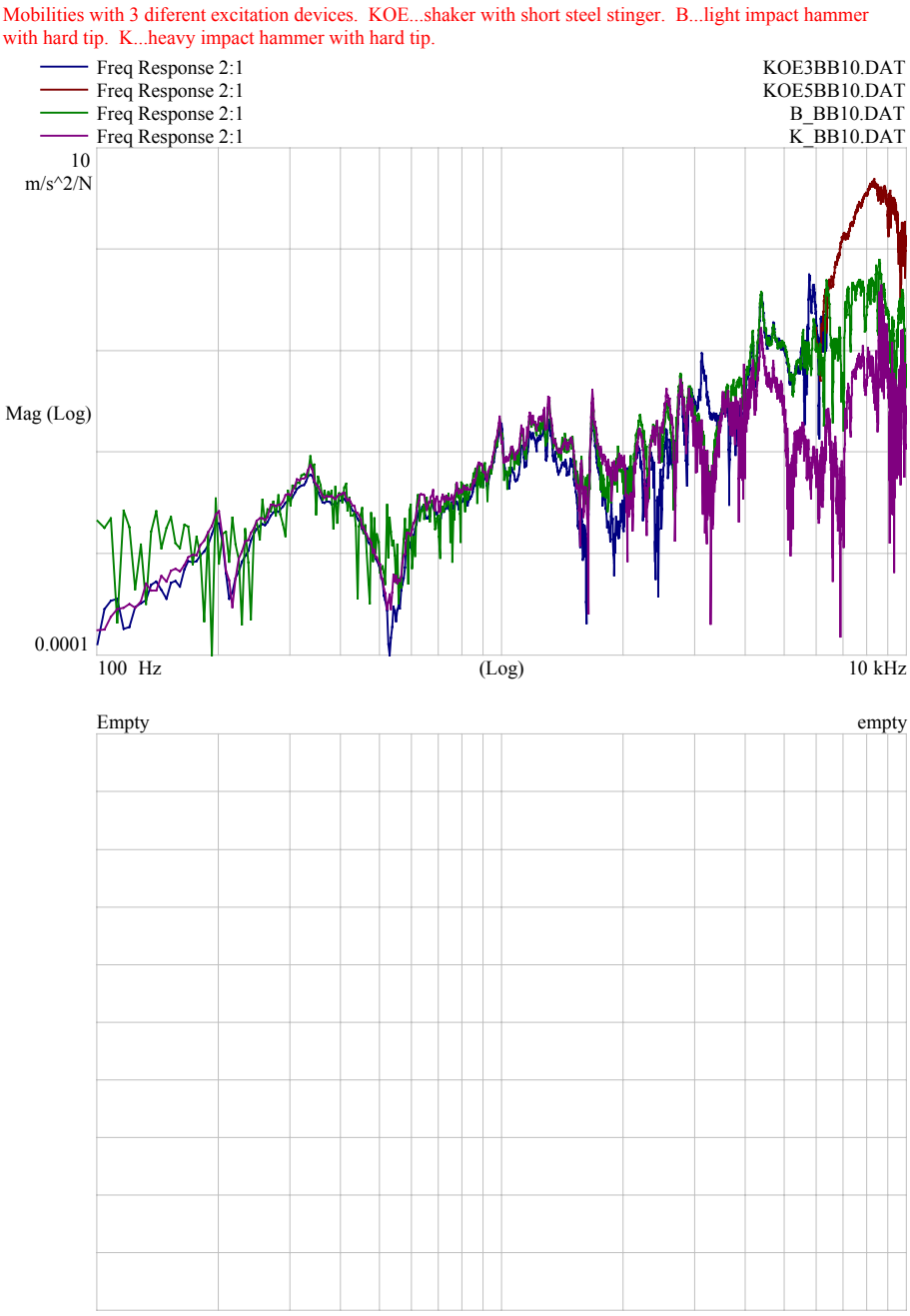

Figure 22. Driving-point mobility (logarithmic axis) with three excitation devices (lower picture is empty due to feature of graphics) (logarithmic frequency axis).

Driving-point mobility of four excitation points and corresponding coherence are seen in figure 23. Shapes of FRFs were fairly the same but some major differences can also be seen (figure 23). Coherence was excellent between frequencies from 300 Hz to 450 Hz as well as from 4000 Hz to 5000 Hz. Coherence was fairly good at some other frequencies too but also very poor at some frequencies (figure 23). Poor coherence will deteriorate the estimation of power flow in some extent.

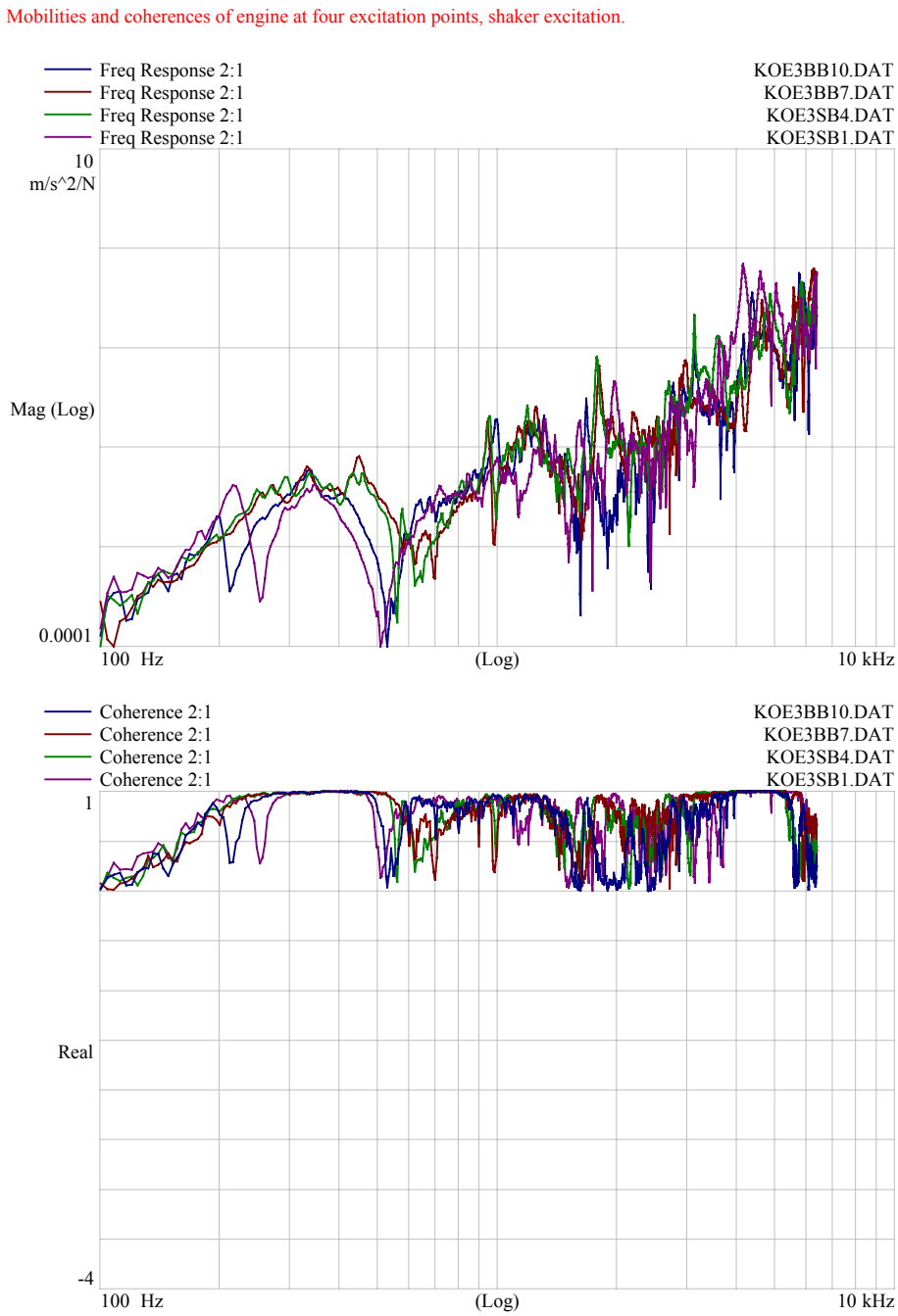

Figure 23. Driving-point mobility (upper, logarithmic axis) and coherence (lower, linear axis) of four excitation points; (logarithmic frequency axis in all).

5.2.4 Response during test runs

Measurements under four operational loads were carried out at test site of Wärtsilä in Turku 16.7.2001. Operational loads of the engine were 85%, 90%, 100% and 110%. Running speed of the engine was 514 rpm. Vertical response in ten measuring points, both in engine and in engine foundation, is seen in figure 24 when engine load was 85%. Vibration was highest between frequencies from 200 Hz to 1000 Hz and was below level of 10 m/s², rms.

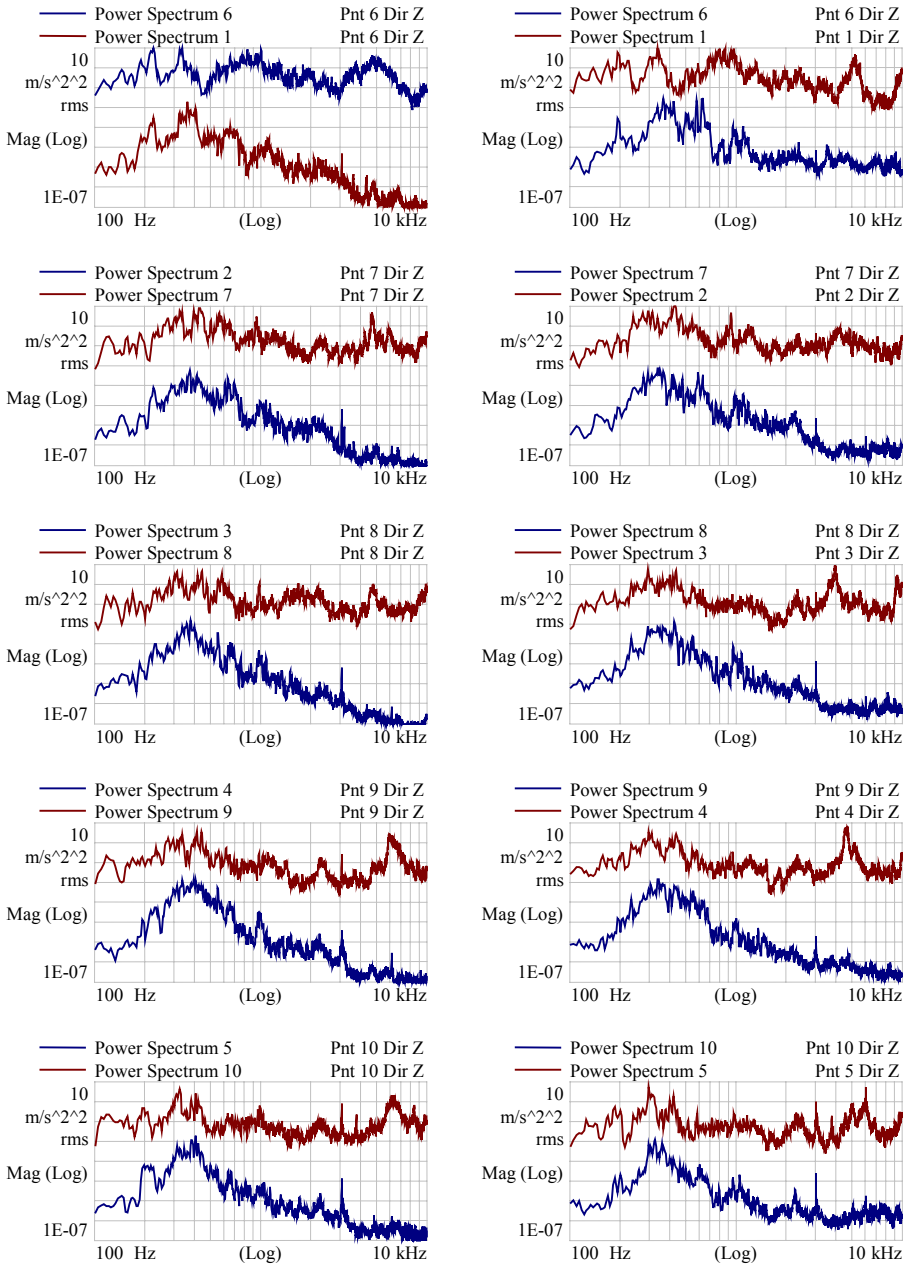

Figure 24. Vibration acceleration spectra (m/s², rms, logarithmic axes) at measuring points 1...10 with operational load of 85% during test run; engine (upper curves) and engine foundation (lower curves); MP 1-5 (pictures on left), from up to down, respectively and MP 6-10 (pictures on right), from up to down, respectively.

6 Analysis

All data acquisitions were done with sampling frequency of 32.768 kHz, which gives usable frequency range from zero to 12.8 kHz. FRFs were analysed on-line during data acquisitions in the field using Hewlett-Packard signal analyser (HP 3566A/67A, version A.04.03). Further analyses were done with LMS Cada-X software (version 3.5.D SL2). These further computations, i.e. computation of power flow according to the equation (2), were done using complex block data computation feature of application software named Time Data Processing Monitor (TMON) of Cada-X.

6.1 Power calibration

Power calibration was done as follows. Spatially averaged velocity, first term in equation (2), was calculated from measured eight velocities during shaker excitation. Injected power was calculated from measured force and velocity at driving-point as

$$P_i = \tfrac{1}{2} \mathrm{Re}\,(\mathbf{F_i}\, \mathbf{v_i}^*) \qquad (3)$$

where P_i is injected power, Re ( ) is real part of ( ), $\mathbf{F_i}$ is measured complex force amplitude, $\mathbf{v_i}^*$ is complex conjugate of measured complex velocity amplitude $\mathbf{v_i}$.

Latter parenthetical term in equation (2) was estimated as a quotient of injected power and average velocity. Four driving-points were used and therefore four proportionality functions, denoted as Re(ά), were calculated (figure 25).

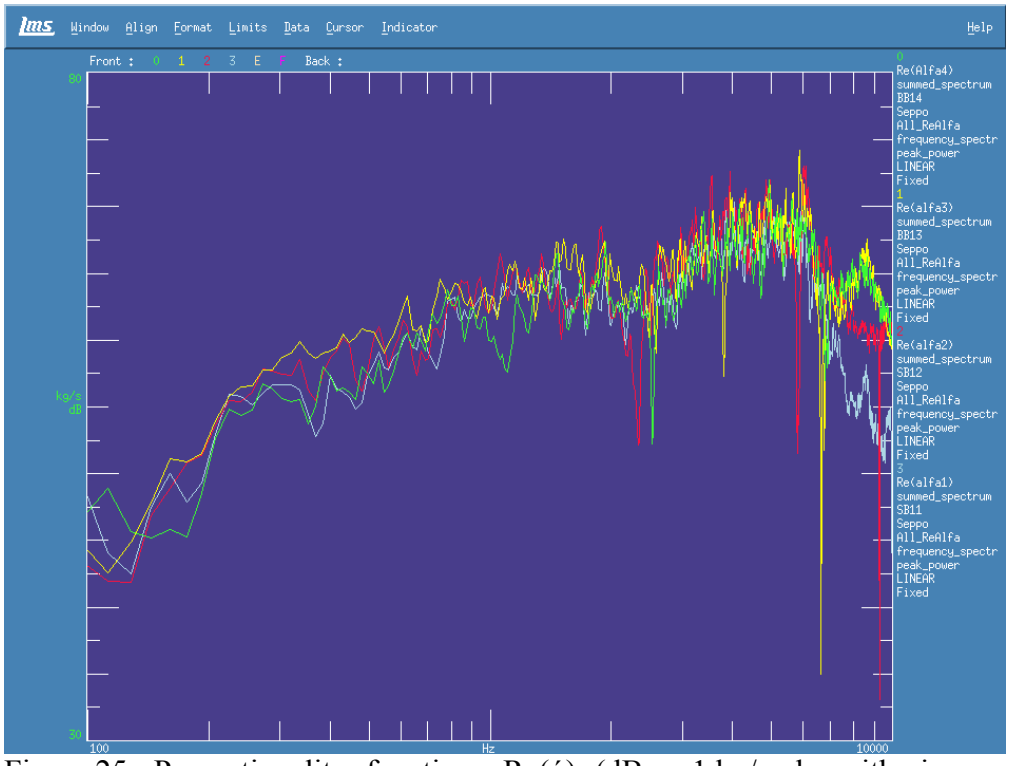

Figure 25. Proportionality functions Re(ά) (dB, re 1 kg/s, logarithmic axes) for different driving-points (note: kg/s = Ns/m).

Four proportionality functions were roughly the same up to the frequency of 6.5 kHz (figure 25) which was earlier concluded to be the upper limit of usable frequency range (figures 6-10).

7 Results

Vibrational power calculated using four different proportionality functions for load of 85% are seen in figure 26 and powers for different loads are seen in figure 27.

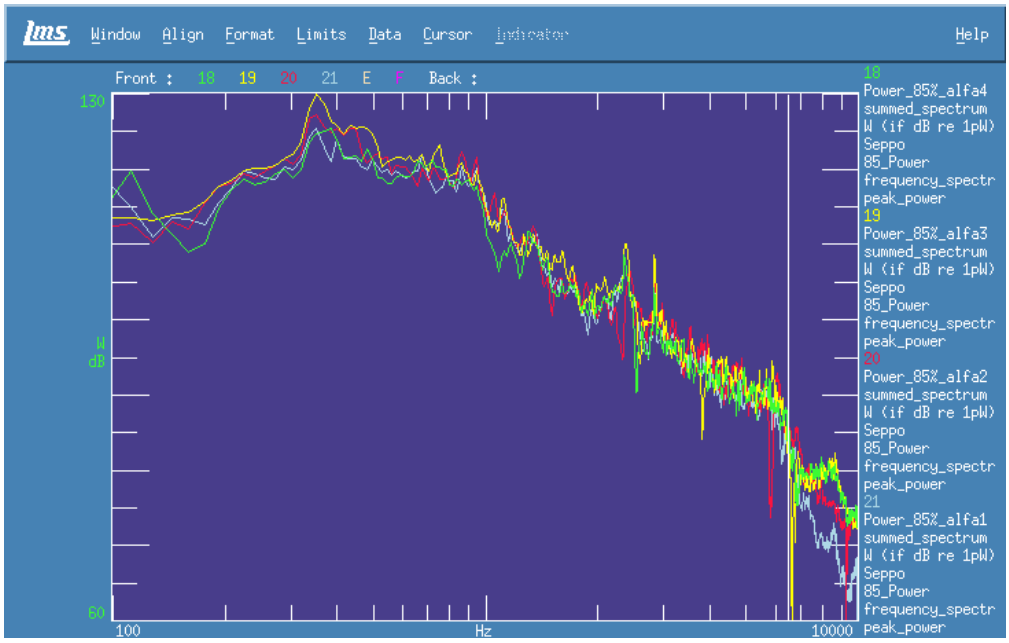

Figure 26. Vibrational power (dB, re 1e-12 W, logarithmic axes) at load of 85% during sea voyage calculated with four different proportionality functions Re(ά).

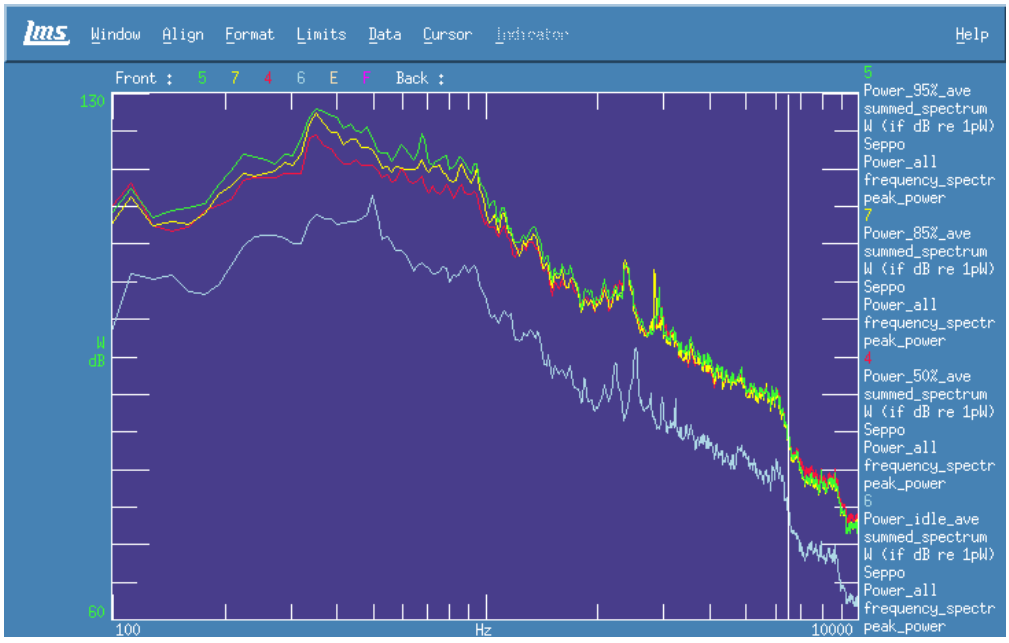

Figure 27. Average vibrational power (dB, re 1e-12 W, logarithmic axes) during sea voyage at loads of 95%, 85%, 50% and idling, from upper most to lowest curve (green, yellow, red and blue curve), respectively.

Vibrational power calculated using equation (2) and four different points for load of 85% are seen in figure 28 and average power for different loads are seen in figure 29.

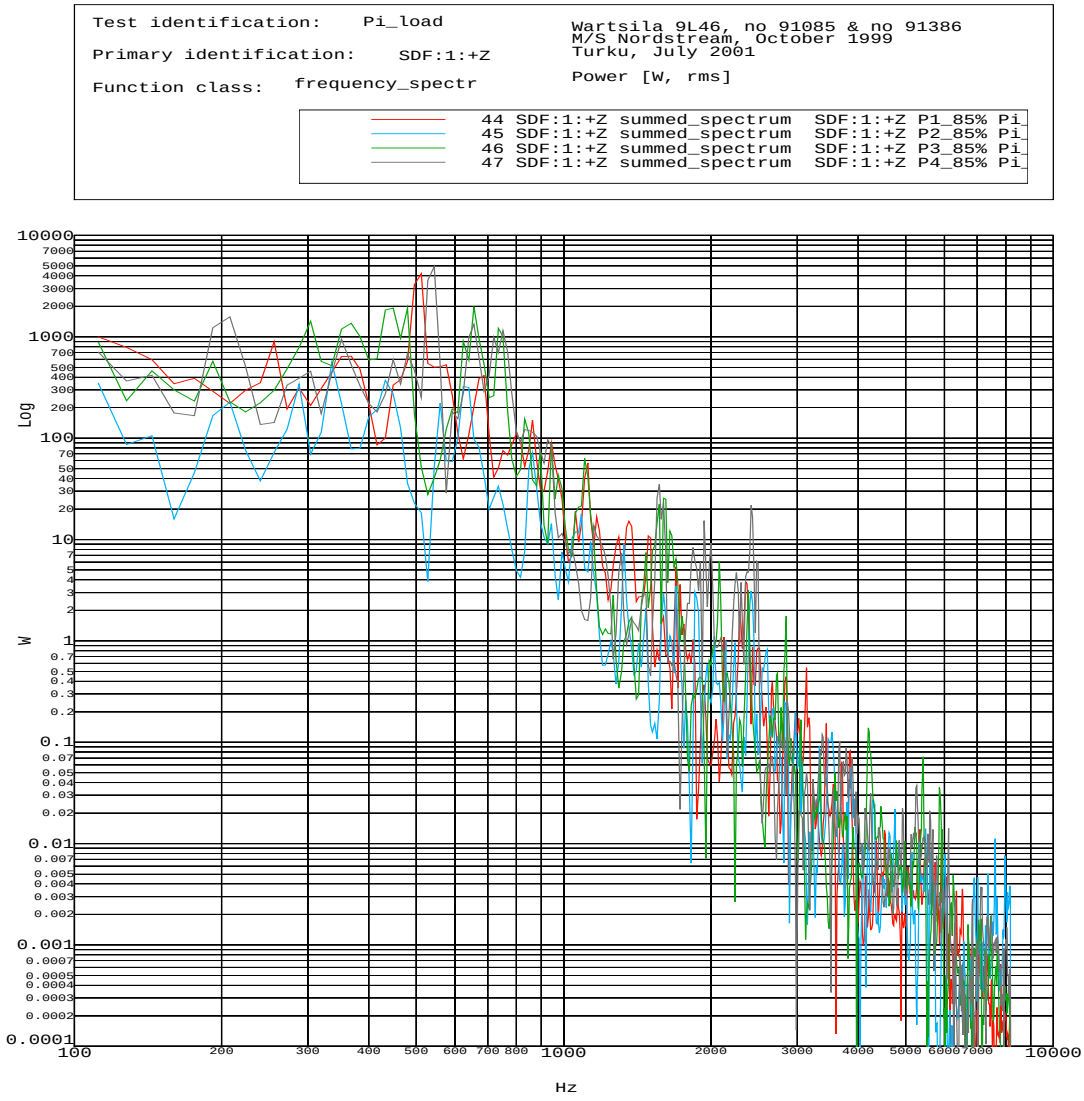

Figure 28. Vibrational power (W, logarithmic axes) at load of 85% during sea voyage calculated using equation (2) and four different driving-points.

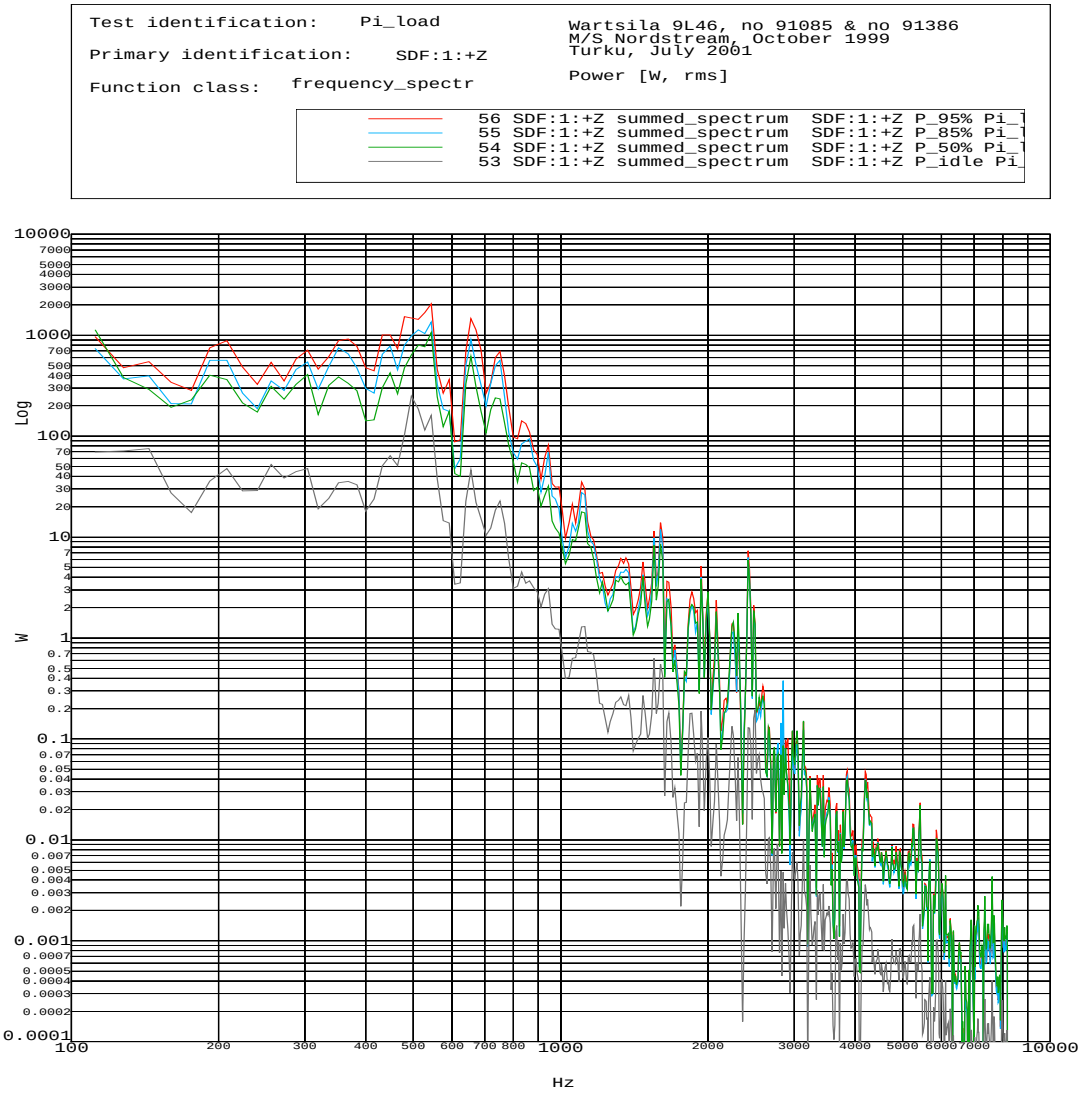

Figure 29. Average vibrational power (W, logarithmic axes) during sea voyage at load of 95%, 85%, 50% and idling from upper most curve to lowest curve, (red, violet, green and black) respectively, calculated using equation (2).

Average vibrational power for load of 85% calculated using both proportionality functions and equation (2) are seen in figure 30 for comparison. Corresponding average vibrational powers for idling, load of 50% and 95% are seen in figures 31, 32 and 33, respectively.

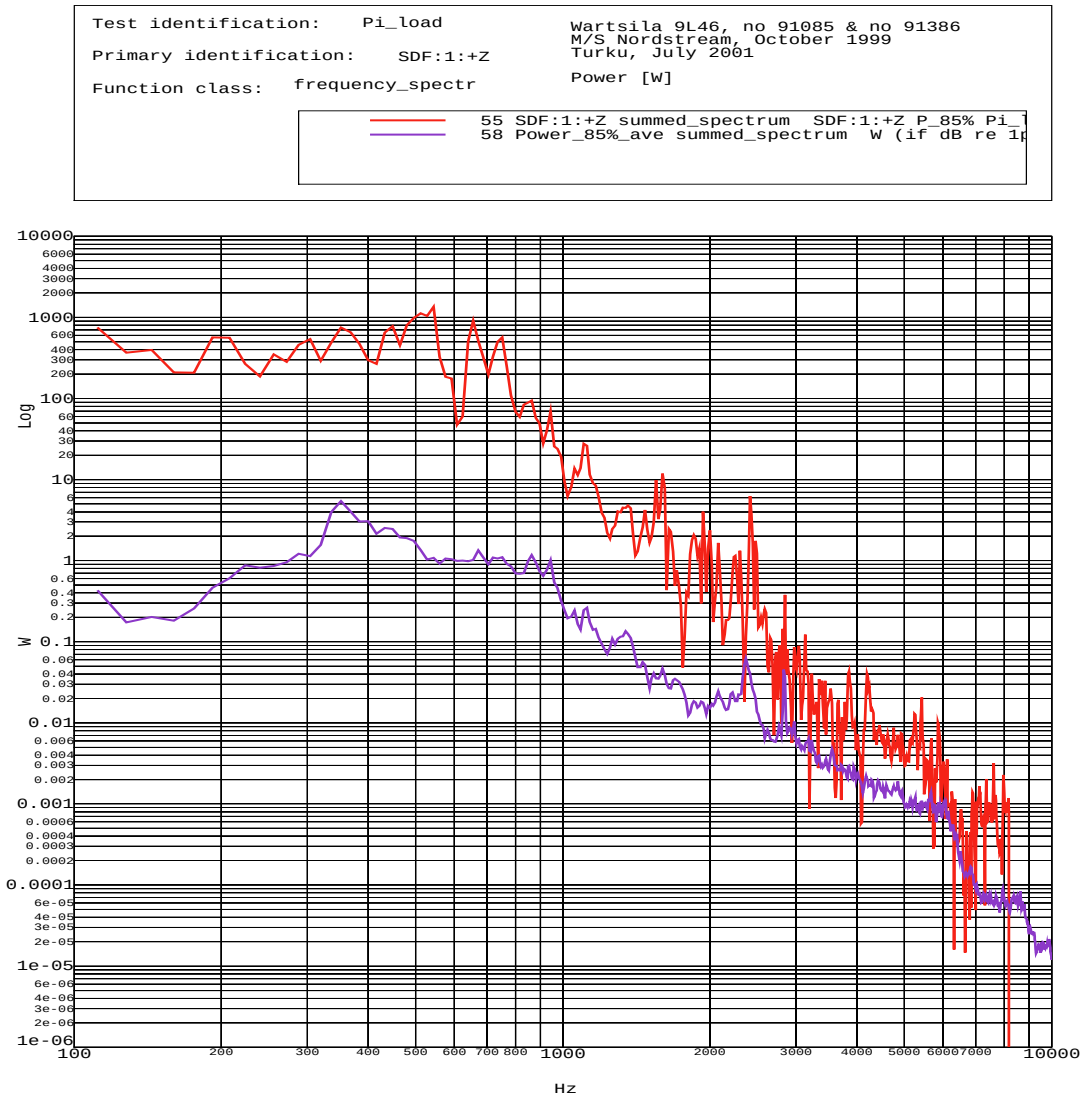

Figure 30. Average vibrational power (W, logarithmic axes) at load of 85% during sea voyage calculated using equation (2) (red curve) and using proportionality functions (violet curve).

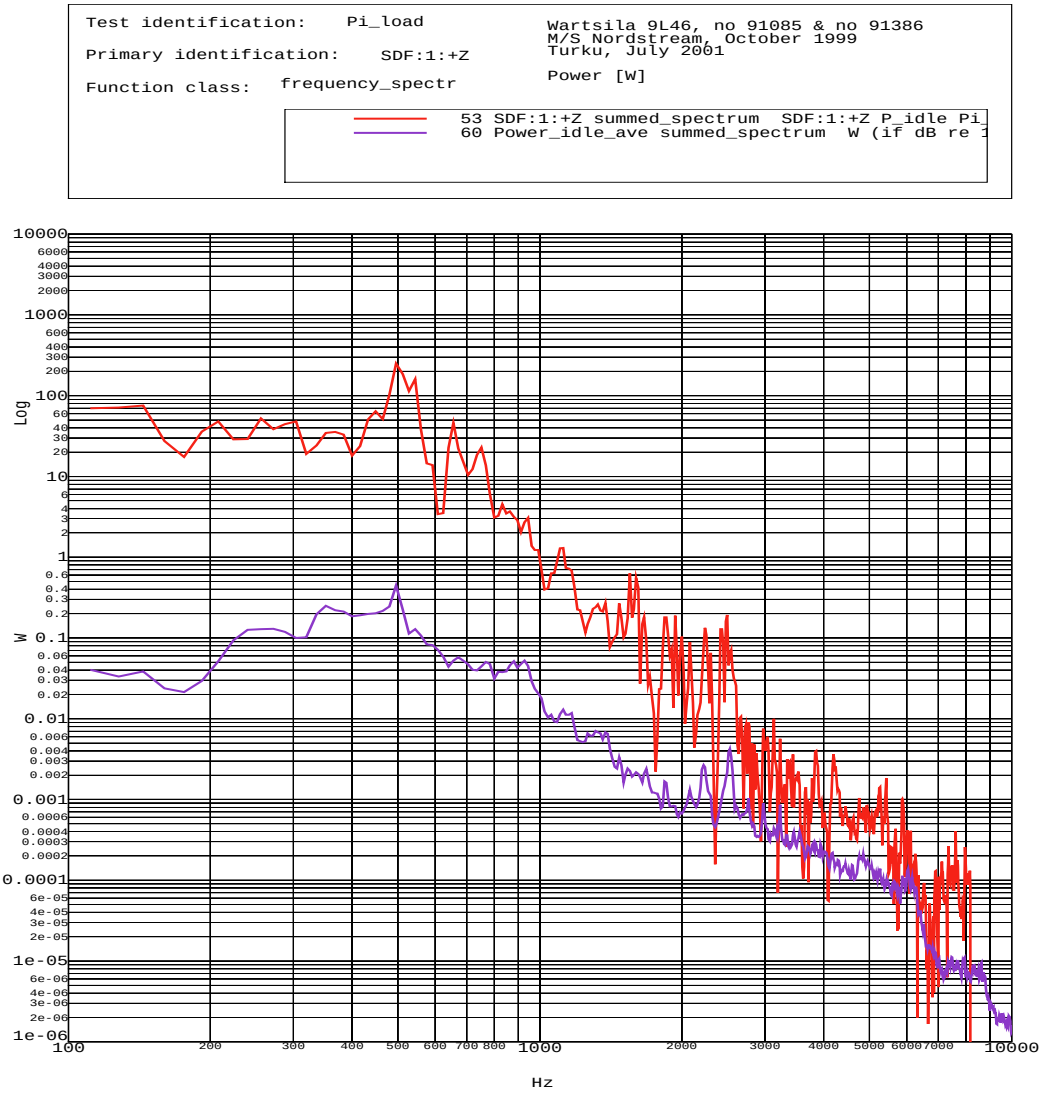

Figure 31. Average vibrational power (W, logarithmic axes) at idling calculated using equation (2) (red curve) and using proportionality functions (violet curve).

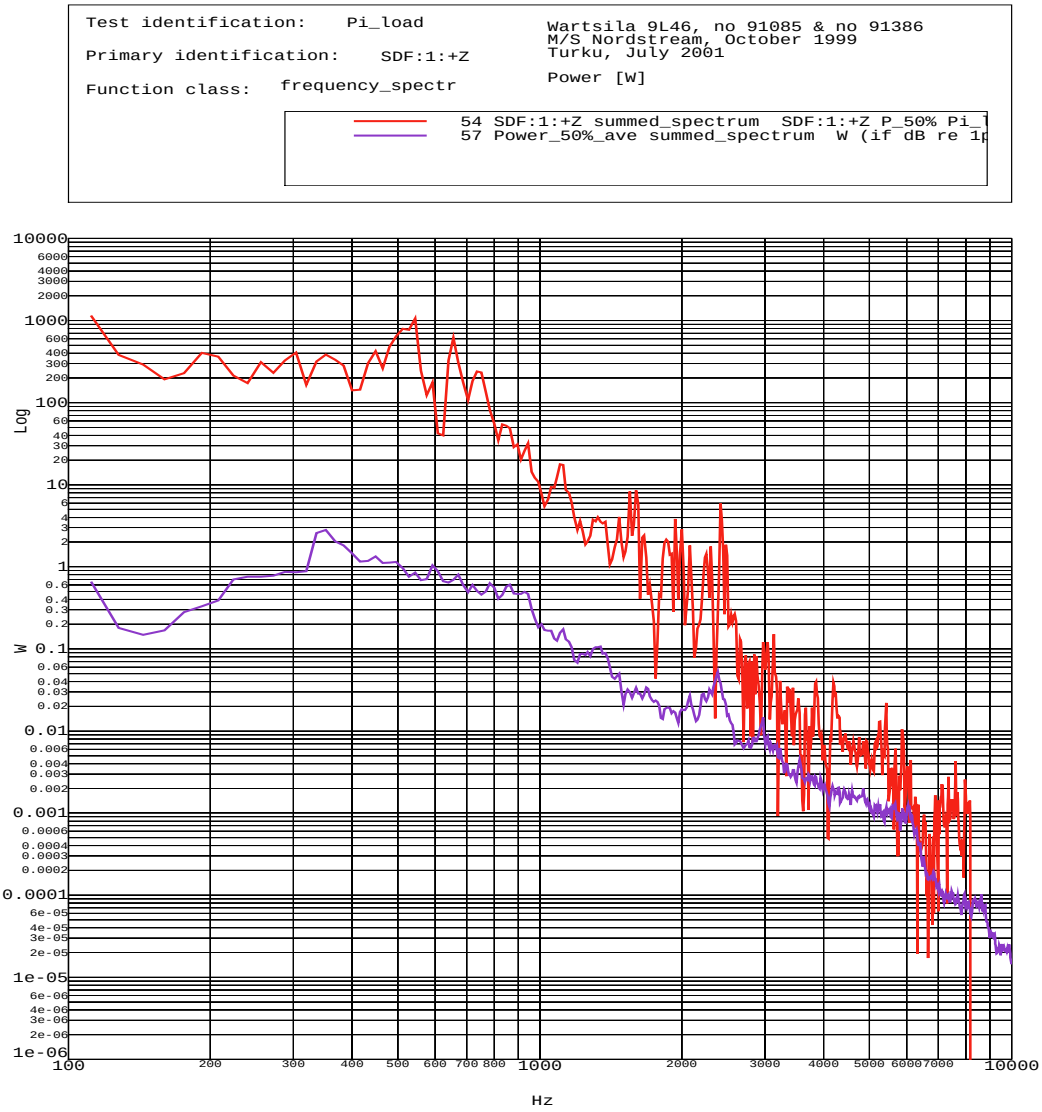

Figure 32. Average vibrational power (W, logarithmic axes) at load of 50% during sea voyage calculated using equation (2) (red curve) and using proportionality functions (violet curve).

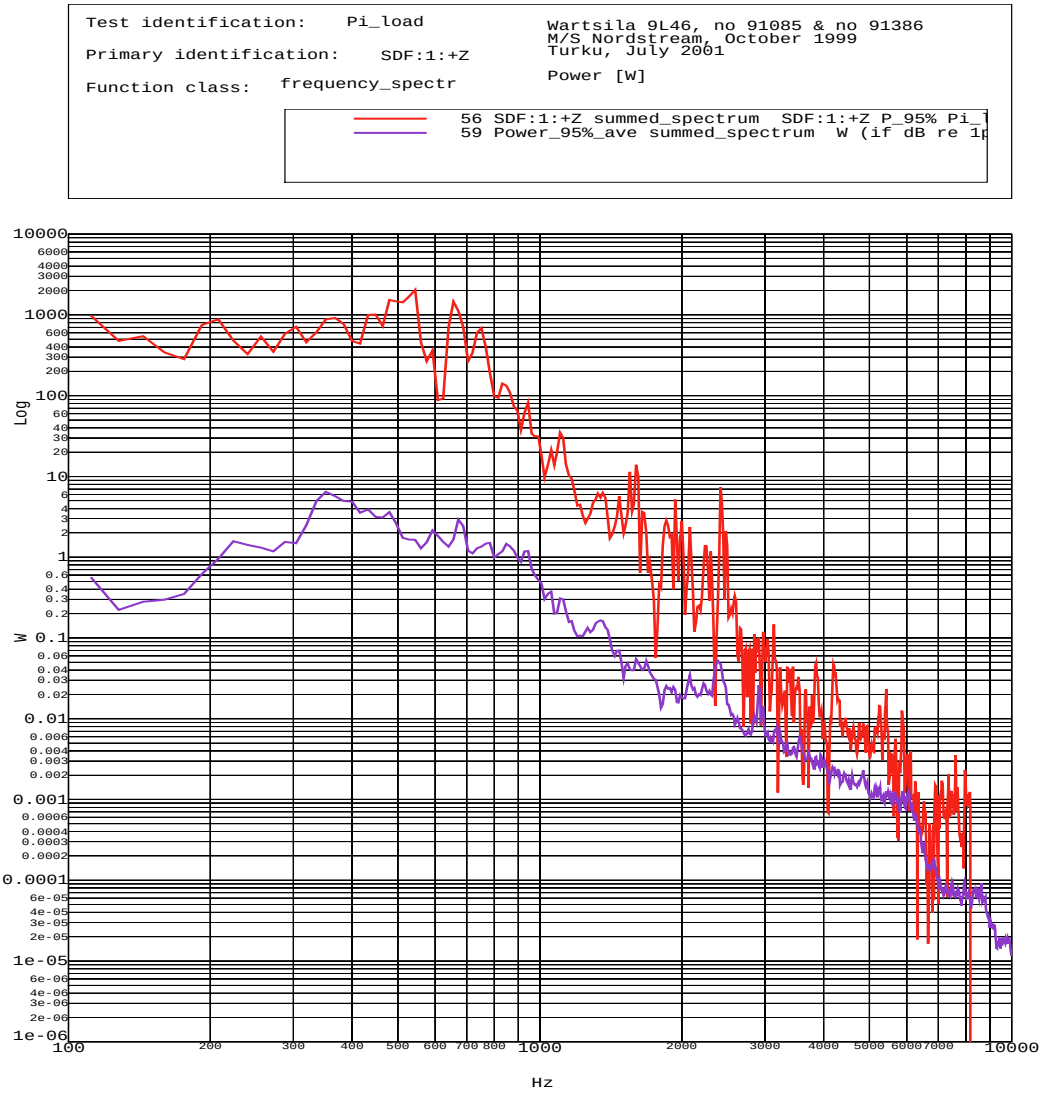

Figure 33. Average vibrational power (W, logarithmic axes) at load of 95% during sea voyage calculated using equation (2) (red curve) and using proportionality functions (violet curve).

8 Discussion

Measurements of force and driving-point mobility during shaker excitation in the ship showed that results could be expected to be valid inside the frequency range from 200 Hz to 6000 Hz. However, spectra of excitation force within this frequency range were far from flat spectra and force was near to background noise at some frequencies. Vibration response in far field was also very close to the background noise at the farthermost measuring points. Frequency range could be increased using light impact hammer with hard tip and heavy impact hammer with soft tip, from high-frequency end and low frequency end, respectively. However, best compromise would be use of powerful shaker together with ideally rated force transducer because then calculations could be done in a consistent way, i.e. simultaneously at all frequencies. However, use of two or more frequency bands might be needed to achieve adequate vibration level in response points.

Proportionality functions Re(ά), determined using four driving-points, were quite equally shaped and roughly the same up to the frequency of 6500 Hz. Vibrational powers calculated

using these proportionality functions differed from each other only by few decibels but also differences as large as 10 dB were seen at some frequencies. This lead to the fact that vibrational power spectra calculated at different engine loads criss-crossed each other. However, use of average proportionality function lead to the fact that vibrational power spectra were in ascending order with ascending engine load up to the frequency of 1000 Hz. Above 1000 Hz vibrational powers were nearly the same regardless of engine load. Use of one-third octaves might give more consistent results comparing to narrow band analyses used in this study. With one-third octaves local effects due to reverberation around measuring points will be smoothed out in an appropriate way.

Vibrational powers calculated using equation (2) and four driving-points were also quite equally shaped and roughly the same up to the frequency of 6500 Hz. Other comments (see above) on ascending order of power spectra with ascending engine load were also true when powers were calculated using equation (2).

Vibrational power calculated using proportionality functions Re(ά) and using equation (2) differed from each other. This difference was quite large at low frequencies but decreased with ascending frequency; difference was finally nearly zero at frequency of 6000 Hz. At the moment there is no distinct explanation for this difference. One reason might be the fact that the vibration source, the diesel engine, was already installed during measurements. Therefore this method gives an approximation of real proportionally function and finally only a rough estimation for the vibrational power. However, this difference might be partially resulted from the use of relatively small shaker comparing to the relatively large and heavy measuring target. Other reason is that during sea voyage both main engines were running at same speed and same load during measurements i.e. the second main engine as well as other auxiliary equipment of the ship were additional vibration sources in the system. Other possible reasons might be cross-coupling effect which is ignored in the method and the fact that driving-point mobility was not measured from the very same engine. Also locations of driving-points in these engines were not the same, due to the practical valid reasons during measurements. Calculation procedure used in this study is not checked with well known synthetic data; therefore inaccuracy in the calculation procedure is not entirely ruled out.

9 Conclusions

Method presented by Ohlrich [2] was applied to ship main engine and ship hull in full-scale. Vibrational power transmission from main engine to ship hull was calculated from measured vibration data, i.e. using driving-point mobility, transfer mobility and vibration velocities in the "far-field". Vibrational power calculated using proportionality functions Re(ά) and using equation (2) has discrepancy which cannot be fully explained. Probably results could be improved by optimising excitation equipment for large and heavy structures, which will rise responses in the "far-field" more clearly above background level. However, the method seems to be promising but further experiments are needed to find out the confidence of the method in the case of large structures.

Acknowledgements

Bore shipowners and Aker Finnyards Oy enabled measurements in the ship. Kari Kyyrö from Aker Finnyards arranged measuring schedule in Rauma before sea voyage. Personnel of Aker Finnyards in Rauma helped to install measuring equipment on board. Chief Engineer Gerrit

de Haan and Captain Ernest van den Brink of M/S Nordstream were very co-operative and vibration measurements were done in good and steady conditions during sea voyage. Wärtsilä Finland Oy enabled measurements of the resiliently mounted engine. Petri Aaltonen from Wärtsilä arranged measuring schedule in Turku. Personnel of Wärtsilä at test site in Turku were very helpful and took care that engine was in steady operating state during measurements. Vesa Nieminen from VTT took part in and took care of measuring equipment during measurements in Rauma and during sea voyage. Pertti Hynnä from VTT took part in measurements both in Rauma and in Turku.

References

[1] Hynnä, P. Vibrational Power Methods in Control of Sound and Vibration. Espoo: Technical Research Centre of Finland, VTT Industrial Systems, 2002. 106 pp. (Research Report, No BVAL37-021229).

[2] Ohlrich, M. In-situ estimation of structural power transmission from machinery source installations. Sixth International Congress on Sound and Vibration, 5-8 July 1999, Copenhagen, Denmark, pp. 2149-2160.